# Distribution and Synaptic Localization of Immunocytochemically Identified NMDA Receptor Subunit Proteins in Sensory-Motor and Visual Cortices of Monkey and Human

G. W. Huntley,[1] J. C. Vickers,[1] W. Janssen,[1] N. Brose,[3] S. F. Heinemann,[3] and J. H. Morrison[1,2]

[1]Fishberg Research Center for Neurobiology and [2]Department of Geriatrics and Adult Development, The Mount Sinai School of Medicine, New York, New York 10029-6574, and [3]Neurobiology Laboratory, The Salk Institute for Biological Studies, La Jolla, California 92037

NMDA receptors are composed of multiple receptor subunit proteins, of which NMDAR1 appears to be a critical component for normal receptor function (Nakanishi, 1992). In this study, quantitative immunocytochemical methods were used at the light and electron microscopic levels to localize NMDAR1 subunits in the primary motor (M1) and somatic sensory (S1) cortex of monkeys, and in the primary visual cortices (V1) of monkey and human. Three principal features of NMDAR1 subunit organization were examined in detail in the monkey cortex: (1) the laminar and cellular distribution patterns, relying in part on double-labeling paradigms with the calcium-binding proteins parvalbumin (PV) and calretinin (CR) as markers for discrete subpopulations of GABAergic interneurons; (2) the codistribution of NMDAR1 subunits with non-NMDA ionotropic receptor subunits; (3) a quantitative assessment of the percentages of asymmetrical synapses in layers II/III, IV, and V/VI that were NMDAR1 immunoreactive.

In monkey M1, S1, and V1, NMDAR1 immunoreactivity was present in all layers, localized primarily to large numbers of pyramidal cell somata and proximal apical dendrites, to presumptive spiny stellate cells in layer IV of V1, and to the vast majority (~80–90%) of PV-immunoreactive cells. By contrast, NMDAR1 immunoreactivity was present in only a very small percentage of the CR-immunoreactive cells (~6–9%). Colocalization with non-NMDA receptor subunits showed that all cells (100%) that contained GluR2/3 subunits were also NMDAR1 immunoreactive. In addition, the complete codistribution of GluR5/6/7 subunits with GluR2/3 subunits suggests, indirectly, that all GluR5/6/7-immunoreactive cells are also NMDAR1 immunoreactive. The laminar and cellular distribution patterns of immunostaining in human V1 were very similar to those in monkey V1.

Electron microscopy of monkey sections confirmed an extensive dendritic and synaptic localization of NMDAR1 subunits. Labeling of synapses was present on asymmetrical postsynaptic densities associated with both dendritic shafts and spines. In supragranular layers of V1, a greater percentage of asymmetrical synapses were NMDAR1 immunopositive (44%) in comparison to layer IVCβ (34%) or deep layers (19%). In contrast, in area 3b of S1, the percentage of labeled synapses was greatest in layer IV (45%) in comparison to superficial (26%) and deep (37%) layers, while in M1, the percentages of labeled synapses were similar between superficial (46%) and deep (40%) layers.

Taken together, these data indicate that NMDAR1-immunoreactive cells in neocortex represent a morphologically, functionally, and neurochemically heterogeneous population. In addition, the NMDAR1-immunopositive synapses represent a major proportion of the asymmetrical synapses in primary sensory and motor cortex, and have a distribution suggesting that in primates, they play a major role in mediating a diverse set of excitatory afferents.

[Key words: excitatory synaptic transmission, excitatory amino acid receptors, cortical circuitry, primate, immunocytochemistry, electron microscopy, NMDAR1]

NMDA receptors comprise one of the three principal classes of ionotropic excitatory amino acid (EAA) receptors in the CNS (Nakanishi, 1992), and have long been thought to play key roles in the cellular mechanisms underlying both activity-dependent synaptic plasticity (Collingridge and Bliss, 1987; Kleinschmidt et al., 1987; Constantine-Paton et al., 1990; Fox and Daw, 1993; Kirkwood et al., 1993) and EAA-induced toxicity and cell death (Rothman and Olney, 1987; Choi, 1988). These roles derive, in part, from the unique voltage-dependent nature of NMDA receptor channel opening (Mayer et al., 1984; Nowak et al., 1984), the longer duration and latency of onset of NMDA-induced synaptic currents in comparison to those induced by non-NMDA receptor activation (Ascher and Nowak, 1987), and the Ca²⁺ permeability of the NMDA receptor channel (MacDermott and Dale, 1987).

More recently, however, it has become apparent that NMDA receptors may also contribute to synaptic transmission of sensory information in a context not necessarily associated with "plasticity." For example, brief cutaneous stimulation leads to

both non-NMDA and NMDA receptor–dependent responses in the dorsal horn of the spinal cord in monkeys (Evans and Long, 1989; Dougherty et al., 1992) and in the ventrobasal thalamic complex (Salt, 1986; Salt and Eaton, 1989) and the first somatic sensory cortex (Armstrong-James et al., 1993) of rats. In the visual cortices of cats and kittens, patterned visual stimulation results in NMDA and non-NMDA receptor–dependent responses in subsets of cortical neurons (Tsumoto et al., 1987; Fox et al., 1989; Miller et al., 1989). While it is generally thought that alleviation of the voltage-sensitive magnesium block of NMDA receptor channels is dependent on prior membrane depolarization due to the faster kinetics of non-NMDA receptor activation (Mayer et al., 1984; Nowak et al., 1984), the data imply an additional, more fundamental role for NMDA receptors in sensory neurotransmission than previously assumed. Thus, NMDA receptors may be an essential component of a large number of the excitatory circuits upon which normal cerebral cortical function is dependent.

NMDA receptors are composed of families of multiple subunit proteins, and in this respect resemble the non-NMDA ionotropic receptors (reviewed in Gasic and Hollmann, 1992). NMDAR1, which was the first subunit identified (Moriyoshi et al., 1991), is present in many neurons throughout a large number of regions in the CNS (Nakanishi, 1992), and can exist in several isoforms apparently generated by alternative splicing (Anantharam et al., 1992; Durand et al., 1992; Hollmann et al., 1992; Nakanishi et al., 1992; Sugihara et al., 1992). A second family of structurally and functionally related NMDA receptor subunits has been identified (NMDAR2, A–D), the corresponding mRNAs of which show a more restricted distribution throughout the CNS in comparison to that of NMDAR1 (Kutsuwada et al., 1992; Meguro et al., 1992; Monyer et al., 1992). Expression studies in *Xenopus* oocytes have suggested that functional NMDA receptor complexes are composed of heteromeric assemblies of discrete subunit proteins in which NMDAR1 subunits are an essential component (Kutsuwada et al., 1992; Meguro et al., 1992; Monyer et al., 1992; Nakanishi, 1992). Thus, the localization of NMDAR1 subunits is likely to reflect the majority of—if not all—NMDA receptor complexes (Nakanishi, 1992).

The present study represents one in a series of studies aimed at elucidating the anatomical organization of ionotropic glutamate receptor subunits in the primate cerebral cortex by using immunocytochemical probes to individual EAA receptor subunits. Our previous investigations in monkeys have shown a high degree of specificity in the regional, laminar, cellular, and neurochemical organization of subunits of the AMPA/kainate (GluR1–3) and kainate (GluR5–7) families (Huntley et al., 1993; Vickers et al., 1993), some features of which have also been demonstrated in the cortices of other species (Rogers et al., 1991; Petralia and Wenthold, 1992; Martin et al., 1993). However, no studies to date have examined the laminar and synaptic organization of NMDA receptor subunits, or the codistribution of NMDA and non-NMDA receptor subunits, in primate cortex, although a recent study has examined NMDAR1 subunits in monkey hippocampus (Siegel et al., 1994). Such immunocytochemical data supplement and extend previous studies of NMDA receptor localization in the cerebral cortex, which relied principally on ligand binding autoradiography (reviewed in Young and Fagg, 1990). While autoradiographic studies have been useful for establishing broad regional and laminar patterns of receptor binding, they do not permit the cellular or synaptic res-

olution whereby cell- and/or circuit-specific details of the anatomical organization of NMDA receptors, specific receptor subunits, or splice variants may emerge. Therefore, in the present study, quantitative immunocytochemical methods were used to examine the sensory-motor cortex of the monkey and the visual cortices of human and monkey with respect to the following features of NMDAR1 subunit organization: (1) the laminar distribution of NMDAR1-containing cells; (2) the codistribution of NMDAR1 subunits with non-NMDA receptor subunits or with calcium-binding proteins, which were used as markers of discrete subsets of GABAergic interneurons; (3) the percentages of asymmetrical synapses in specific layers that are NMDAR1 immunoreactive. These areas were chosen since they represent the ones from which most physiological data concerning NMDA receptor function in cerebral cortex have been obtained.

## Materials and Methods

This study was conducted on the brains of six adult cynomolgus monkeys (*Macaca fascicularis*) weighing between 2 and 4 kg, and on a single human biopsy specimen that included part of the primary visual cortex. The treatment of all monkeys was in strict accordance with institutional and NIH guidelines for the care and treatment of laboratory animals. Monkeys were heavily anesthetized with ketamine (25 mg/kg) and Nembutal (30 mg/kg) and perfused transcardially first with cold 1% paraformaldehyde (in 0.1 M phosphate-buffered saline (PBS; pH 7.4) for 1 min, followed by an 8–10 min perfusion with cold 4% paraformaldehyde in PBS. The brains were immediately removed, blocked, and postfixed in 4% paraformaldehyde for an additional 6 hr. Blocks were taken in the frontal plane through the pre- and postcentral gyri and through the occipital lobes, in the sagittal plane through the central sulcus at the approximate level of the forelimb representation, and in a plane tangential to the pial surface through visual cortex (V1) taken from the lateral surface just caudal to the lunate sulcus.

The human biopsy material used in this study was obtained from the Division of Neuropathology, The Mount Sinai Medical Center, as part of a larger block of tissue excised during the course of a neurosurgical procedure to remove a tumor from a 62-year-old patient. The block spanned the border between areas 17 and 18. The sections used in this study were histologically normal, based on the pattern of cellular organization revealed in thionin-stained sections.

*Tissue preparation.* Blocks of monkey tissue were sectioned in one of two ways: one set of blocks was frozen in dry ice after cryoprotection in a graded series of phosphate-buffered sucrose solutions, and sections were cut on a freezing sliding microtome at 20 or 40 μm. These blocks of tissue were used for generating light-microscopic, immunoperoxidase, and double-immunofluorescent preparations. A second set of blocks was cut at 50 μm on a vibratome and used for both light and electron microscopic, immunoperoxidase-labeled preparations. Blocks of the human biopsy material were sectioned at 80 μm on a Vibratome. From all blocks, a series of sections was processed for immunocytochemistry, while all other sections were either processed for cytochrome oxidase histochemistry (Wong-Riley, 1979) or stained with thionin.

*Immunocytochemistry.* The primary antibodies used, the species they were generated in, their working dilutions, and the sources for relevant specificity and characterization data are given in Table 1. The mouse anti-NMDAR1 monoclonal antibody (mAb 54.1) used in the present study was generated against residues 660–811 of the NMDAR1 subunit, which correspond to an intracellular segment located between transmembrane regions III and IV. The specificity of mAb 54.1 has been verified by immunocytochemistry of transiently transfected human embryonic kidney 293 cells and by Western blot analyses of monkey CNS tissue and rat synaptic plasma membranes (Siegel et al., 1994).

For single-labeling experiments, sections were transferred to cold PBS containing 5% nonfat milk powder and primary antibody 54.1, and incubated for 36–72 hr at 4°C. Sections were washed repeatedly, and then processed by the avidin-biotin-peroxidase method using Vectastain ABC kits (Vector Labs, Inc.). Immunoreactivity was visualized by reacting sections with 3,3'-diaminobenzidine (DAB) and hydrogen peroxide. Control sections consisted of replacing the primary antibody 54.1

with nonimmune mouse serum, which yielded only a light, diffuse background labeling.

For double-labeling experiments, sections that had been taken from frozen blocks were incubated for 72 hr in cold PBS containing primary antibody 54.1 diluted 1:250 and simultaneously with one of the following monoclonal antibodies or polyclonal antisera: Ab25, which recognizes AMPA/kainate receptor subunits GluR2/3; and anti-calretinin and anti-parvalbumin (Swant-Swiss Antibodies, Switzerland). In addition, a separate series of sections was incubated simultaneously with mAb 4F5, which recognizes kainate receptor subunits GluR5/6/7, and Ab25. All sections were then processed for immunofluorescence using secondary antibodies of the appropriate FITC-conjugated or Texas red-conjugated, species-specific combinations. Control experiments consisted of omitting the primary antibodies or, to test the specificity of the secondary antibodies, incubating sections with only one of the primary antibodies of each combination, followed by incubation with the secondary antibody appropriate for the primary antibody that had been omitted. Finally, sections were processed for only one primary antibody of each combination, and then examined with the inappropriate filter block to check for artifactual bleed-through of the fluorophores used. At the concentrations used, this was determined to be negligible.

*Electron microscopy.* Sections were cut at 50 $\mu$m on a Vibratome and processed for immunocytochemistry using mAb 54.1 exactly as described above. After reaction with DAB, the sections were postfixed for 1 hr in 1% osmium tetroxide in 7% sucrose, dehydrated, and infiltrated with Araldite resin. After polymerization, sections were viewed under a dissecting microscope and a scalpel was used to excise either smaller pia-to-white matter strips or narrow strips flanking superficial layers (II and III), deep layers (V and VI), and either layer IV (from area 3b) or layer IVC$\beta$ (from V1). The excised pieces were flat embedded in Araldite resin, cut at 50–70 nm, collected on 100-mesh grids, and viewed unstained on a Hitachi 7000 electron microscope. In order to increase contrast, the aperture was set to the smallest opening.

*Data analysis.* Analysis was performed on a Zeiss Axiophot,photomicroscope equipped with an MSP-65 computer-driven stage and a high-sensitivity CCD camera interfaced with a DEC 3100 workstation and a Macintosh II microcomputer. Sections were viewed either under bright-field optics, or under epifluorescence using a 40× Neofluor objective and filter blocks selective for visualizing FITC or Texas red. Immunoperoxidase-labeled cells were plotted and montaged by exporting digital images of overlapping, individual microscope fields and applying morphometry software developed in this laboratory and in collaboration with colleagues at Scripps Research Institute. For the generation of pia-to-white matter maps, labeled cells were assigned to cortical lamina by overlaying digitized images of adjacent thionin-stained sections. The positions of laminar boundaries were drawn exactly as they appeared in the Nissl-stained sections, and were superimposed onto the maps of plotted cells. For the tangential visual cortex sections, labeled cells were assigned to cytochrome oxidase–dense/poor compartments by overlaying digitized images of plotted cells with ones of adjacent sections processed for cytochrome oxidase histochemistry or stained with thionin, using blood vessels and other landmarks common to both sets of sections as guides for alignment. An estimate of the degree of clustering of labeled cell somata was made from tangentially cut sections by first determining the mean density of labeled cells (*D*) and subjecting the plotted distribution of labeled somata to a nearest neighbor analysis (*m*), both relying on standard algorithms. Next, by relating *m* to the mean density (*D*) by the equation $r = 2\sqrt{D}(m)$, the value of *r* reflects the randomness of the distribution such that if $r = 1$, the distribution is considered random, $r > 1$ suggests a nonrandom distribution, and $r < 1$ suggests a clustered distribution (Morrison et al., 1984; Huntley et al., 1993). Determination of cortical areas was based primarily on the criteria of Brodmann (1905).

For quantitative analysis of double-immunolabeled sections, the numbers of single- and double-labeled cells of each combination were determined for each region examined from 10 separate pia-to-white matter traverses from each of two animals.

For the quantitative assessment of immunolabeled synapses, the sections that had been excised to include only superficial layers, deep layers, or layer IV (see above), taken from two monkeys, were viewed and photographed at a magnification of 10,000×. The regions photographed were randomly chosen, but care was taken to select regions in which immunoreactivity was present throughout, thereby ensuring that counts were done on regions in which adequate antibody penetration was evident. Two investigators blind to the area and layer(s) counted unam-

**Table 1. Primary antibodies**

| Antibody | Directed against | Raised in | Working dilution | Specificity or source |
|---|---|---|---|---|
| 54.1 | NMDAR1 | Mouse IgG | 1:500 or 1:250 | Siegel et al., 1994 |
| Ab25 | GluR2/3 | Rabbit IgG | 1:100 | Wenthold et al., 1992 |
| 4F5 | GluR5/6/7 | Mouse IgM | 1:500 | Huntley et al., 1993 |
| 7696 | calretinin | Rabbit IgG | 1:3000 | Swant-Swiss antibodies |
| 9064 | parvalbumin | Rabbit IgG | 1:2000 | Swant-Swiss antibodies |

biguously identified immunolabeled and unlabeled synapses (asymmetrical postsynaptic densities) from photographic prints at a final magnification of approximately 31,000×, based on standard morphological criteria (Peters et al., 1991). Structures not clearly identified were not counted. A total of 1817 synapses were counted from the three areas (M1, area 3b of S1, and V1), and the percentage of the total that were NMDAR1 immunopositive determined for each laminar sample from each region.

## Results

### General light microscopic features and distribution patterns in monkey cortex

NMDAR1 immunoreactivity was present in each of the monkey neocortical areas examined, which included primary motor cortex (M1; area 4), primary somatic sensory cortex (S1; areas 3, 1, and 2), and primary visual cortex (V1; area 17). In vibratome-sectioned material from monkey cortex, intense immunoreactivity was localized to the cell somata and proximal portions of apical and, to a lesser extent, basilar dendrites of pyramidal cells (Figs. 1–3). In many cases, the intensity of the immunoreactivity decreased along more distal apical dendrites (Fig. 1*B,C*), although in many instances, such lightly labeled apical dendrites could still be followed for several hundreds of micrometers from their origin into overlying layers (solid arrows, Fig. 1*B,C*). In other cases, only cell somata were labeled. In all areas, both lightly and more intensely labeled cell somata of all sizes were present (Figs. 1–3). In addition, within the neuropil of most layers, a fine meshwork of thin, randomly oriented immunoreactive fibers was present, as well as numerous segments of thicker, vertically aligned immunoreactive processes that likely correspond to segments of labeled apical dendrites (open arrows, Fig. 1*B,C*). The reaction product present along the processes often had a very punctate appearance, usually interspersed with light and more evenly labeled regions. In the underlying white matter subjacent to layer VI in each of the areas examined, sparsely scattered, well-labeled cells were often present. No axonal or neuroglial cell labeling was apparent.

### Sensory-motor cortex

Immunoreactive cells and processes were present in all layers of monkey sensory-motor cortex (Figs. 1*A*, 2*A*). There did not appear to be any overt differences in the staining patterns between medial and lateral parts of M1 or S1. Throughout the pre- and postcentral gyri, layer I was composed of a plexus of obliquely oriented, lightly labeled fibers in the deeper half of the layer, which in some cases could be seen to extend from the apical dendrites of pyramidal cells (arrowheads, Fig. 2*B*) and,
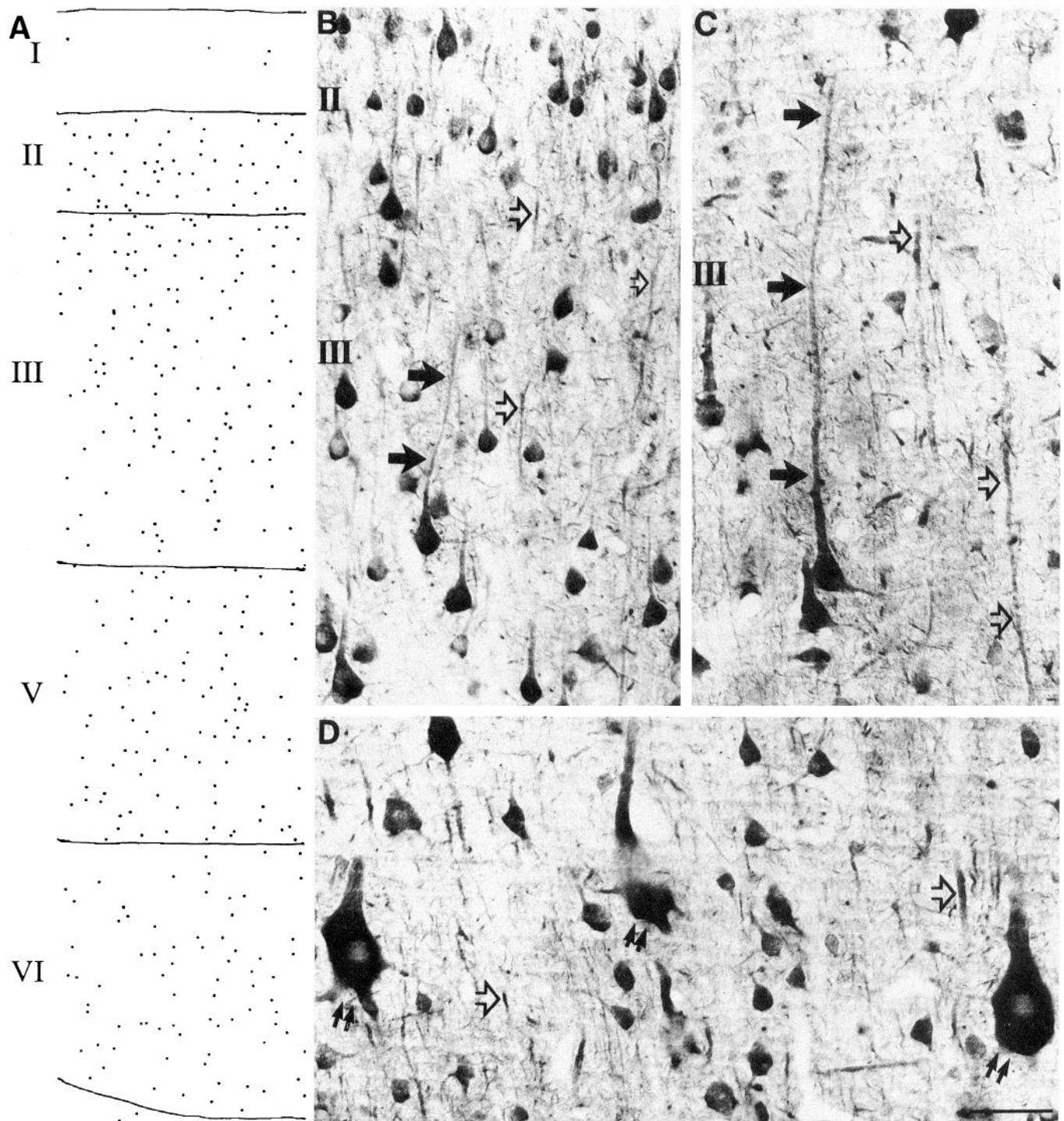
*Figure 1.* NMDAR1 immunoreactivity in M1. *A*, Map showing laminar distribution of immunolabeled somata. *B–D*, Photomicrographs showing numerous small- to medium-sized labeled pyramidal cell somata in superficial layers (*B, C*) and in layer V (*D*), which also possessed very large, labeled Betz cell somata (*double arrows*). In all layers, apical dendrites were labeled, some of which could be traced to their cell body of origin (*solid arrows*), while in the neuropil were numerous segments of thicker labeled fibers (*open arrows*) and finer, obliquely oriented ones. In this and subsequent figures, *Roman numerals* refer to cortical layers. Scale bar, 50 μm.

more superficially, occasional small, lightly labeled cell somata (open arrows, Fig. 2*B*). In motor cortex, layer II through the upper half of layer III appeared slightly more densely packed with labeled somata and segments of vertically oriented processes in comparison with deeper layers (Fig. 1). Layer V was characterized mainly by dense neuropil labeling, the looser overall packing density of labeled somata, and the presence of the

very large, labeled somata of the Betz cells that in some cases, particularly in the anterior bank of the central sulcus, appeared grouped together with intervening spaces between groups composed of smaller labeled somata (Fig. 1*D*). The density of labeled somata in layer VI appeared similar to that in layer V (Fig. 1*A*). Layer VI was composed mostly of small, intensely labeled somata.
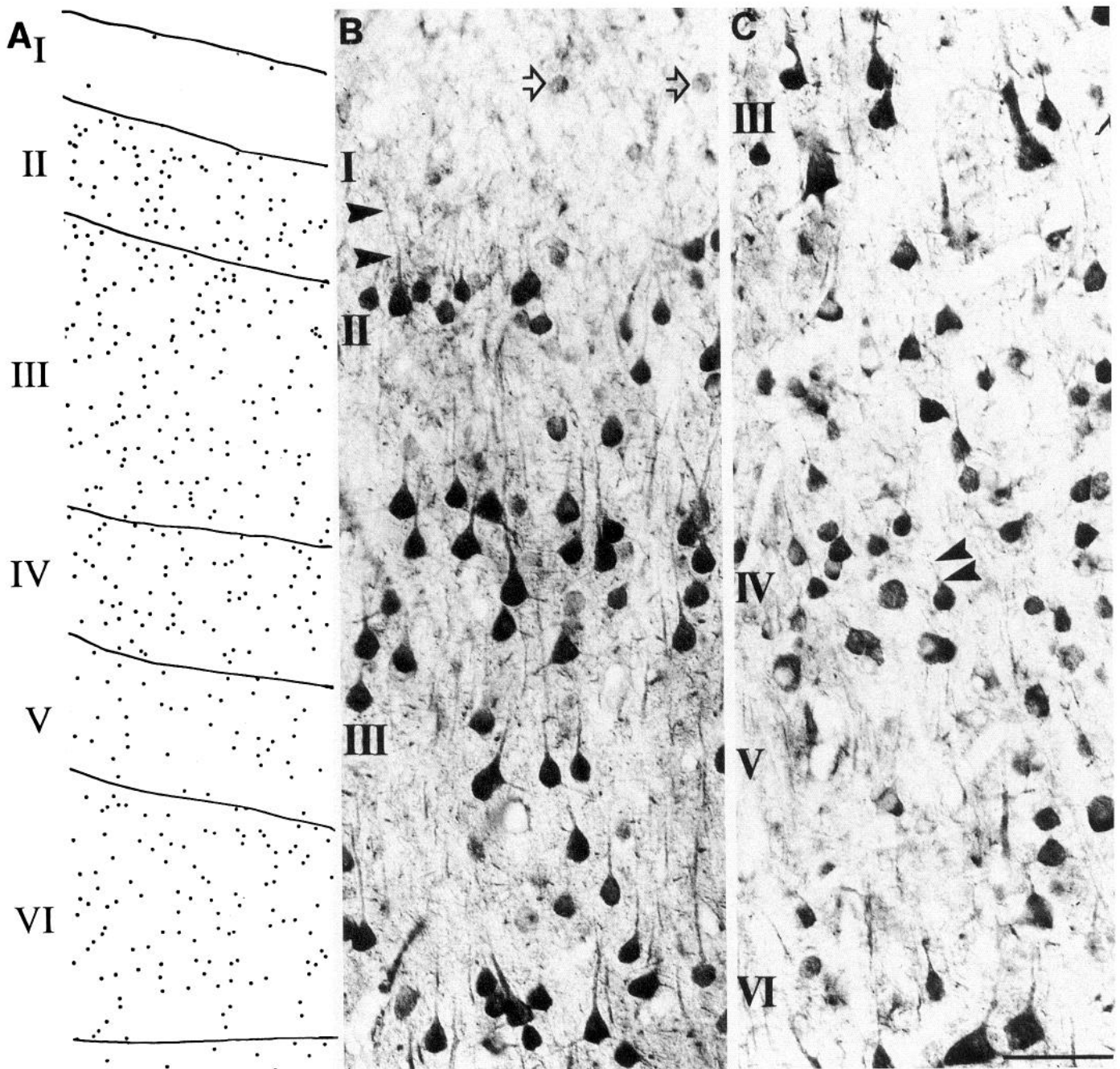
*Figure 2.* NMDAR1 immunoreactivity in S1 (area 3b). Map (*A*) and photomicrographs (*B, C*) show laminar distribution and cellular labeling patterns. Labeled pyramidal cell somata were present in most layers, some of which in layer II gave rise to labeled apical dendrites that could be followed into layer I (*arrowheads in B*). Small, lightly labeled somata were also occasionally present in layer I (*open arrows in B*). In layer IV, many small labeled somata were present, some of which occasionally possessed a faint labeled process (*double arrowheads in C*). Scale bar, 50 μm.

The pattern of labeling was similar across the areas that compose S1 (areas 3a, 3b, 1, and 2), and thus they are described together. Layer II and the upper half of layer III were densely packed with intensely labeled pyramidal cell somata and proximal apical dendrites, and in the neuropil, well-labeled segments of vertically oriented processes (Fig. 2*B,C*). Layer IV possessed some lightly labeled, small, round cell somata, although many were more intensely labeled (Fig. 2*C*). Such cells mostly lacked prominent dendritic labeling, though occasionally, small segments of thin, proximal dendrites could be followed from labeled somata (arrowheads, Fig. 2*C*). In addition, some small

pyramidal cell somata with proximal portions of labeled apical dendrites were present. The density of labeled cell somata in layer V was somewhat lower in comparison to that of layers II and III (Fig. 2*A,C*). Layer VI was more densely packed with medium-sized, well-labeled cell somata and proximal apical dendrites in comparison to layer V (Fig. 2*A*).

### Primary visual cortex

Labeled somata and fibers were present throughout all layers of monkey V1. There did not appear to be any differences in the staining pattern across different retinotopic locations, although
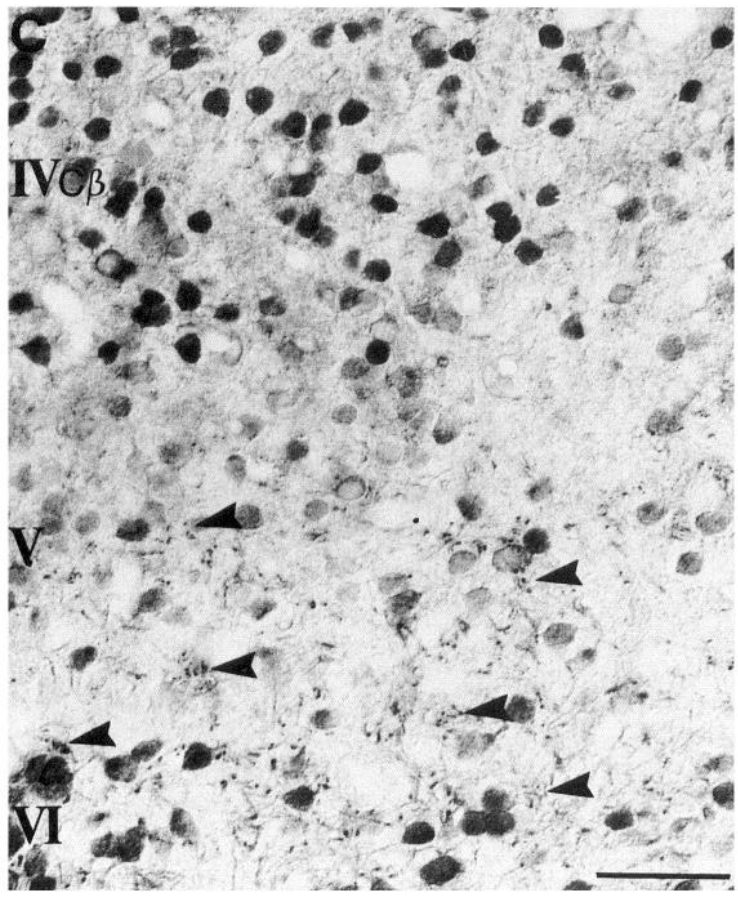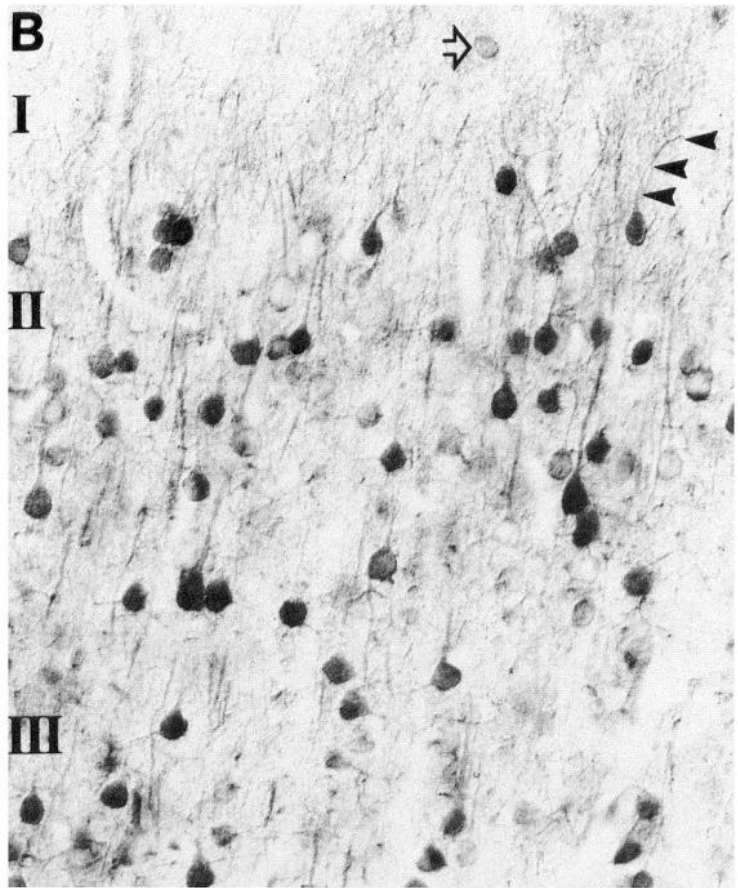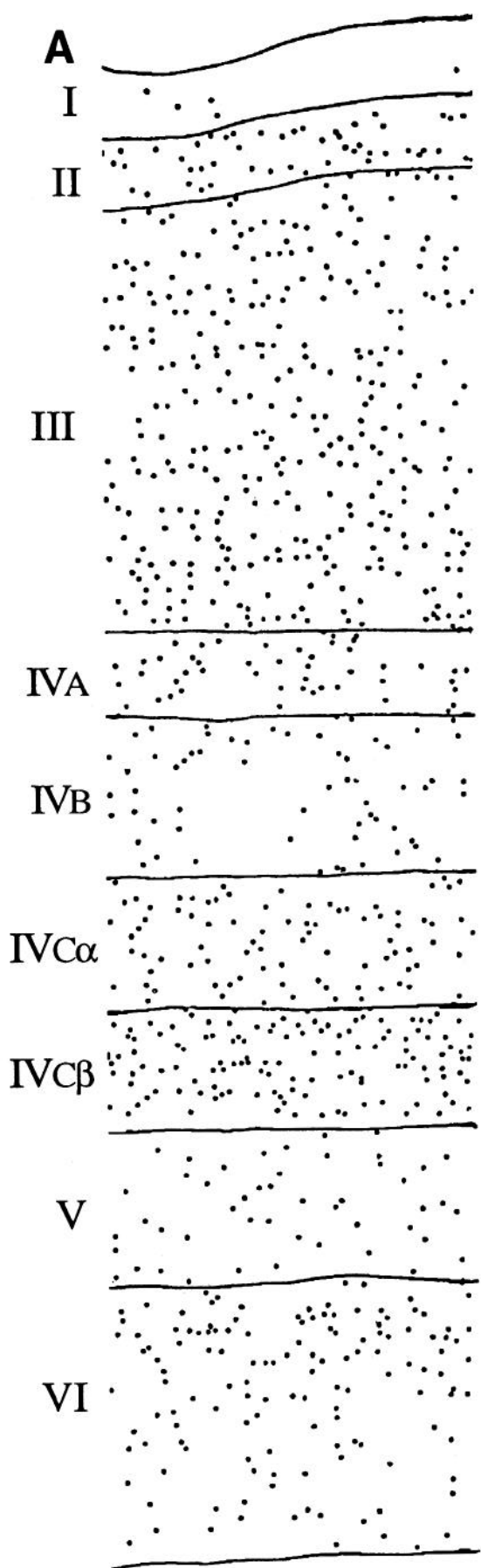
this was not systematically examined. Like sensory-motor cortex, the density of labeling varied by laminae (Fig. 3*A*). The inner half of layer I was composed mostly of thin, randomly oriented labeled processes and very occasional, small, labeled somata (open arrow, Fig. 3*B*). Layers II through III possessed well-labeled, small- to medium-sized pyramidal somata and proximal apical dendrites as well as a rich network of fine neuropil labeling (Fig. 3*B*). In many instances, somata in layer II gave rise to dendrites that could be followed into the inner half of layer I (arrowheads, Fig. 3*B*). Layer IVA possessed labeled somata without prominent dendritic labeling, whose density appeared similar to that in layer III (Fig. 3*A*). In layer IVB, labeled somata were more sparsely distributed (Fig. 3*A*), and often larger and ovoid-shaped in comparison with other layers. Layer IVC possessed densely packed, mostly well-labeled, small round cells that largely lacked any discernible dendritic labeling, interspersed with lightly labeled somata of a similar morphology and fine neuropil labeling (Fig. 3*C*). The density of labeled somata appeared greater in IVC$\beta$ than in IVC$\alpha$ (Fig. 3*A*). Layer V was the least densely and intensely labeled layer in V1 (Fig. 3*A,C*). Layer VIa possessed numerous, well-labeled somata and a rich network of labeled fibers in the neuropil, which, when cut obliquely, appeared as clusters of dots (arrowheads, Fig. 3*C*). Both labeled somata and fibers gradually decreased in density through layer VIb (Fig. 3*A*).

The relationship between the distributions of labeled somata and cytochrome oxidase–rich puffs, which can be used to delineate functionally and connectionally distinct compartments in superficial layers of primate V1 (DeYoe and Van Essen, 1988), was determined from adjacent series of sections cut through layer III in a plane tangential to the pial surface (Fig. 4*A,B*). Although labeled somata often appeared aggregated when viewed in this plane of section, with small, intervening spaces devoid of labeled somata (Fig. 4*A*), there was no overt indication that the immunolabeled cell population was preferentially parcellated to either cytochrome oxidase–rich or cytochrome oxidase–poor compartments (Fig. 4*A–C*). The results of a cluster analysis confirmed that the distribution of labeled somata was likely to be random ($r = 0.92$).

The overall pattern of immunolabeling in the human biopsy sections through V1 was generally similar to that described for monkey V1 (compare Figs. 3, 5). The most notable difference was less neuropil labeling in the human material, although portions of labeled, presumably apical dendrites were still evident in most layers (open arrows, Fig. 5*B*).

### Colocalization

The relationship between the presence of NMDAR1 subunit immunoreactivity and that of immunoreactivities for non-NMDA receptor subunits (GluR2/3) or calcium-binding proteins [calretinin (CR) and parvalbumin (PV)] was examined using double immunofluorescence. Although a detailed description of the pattern of GluR2/3 immunoreactivity in sensory-motor and visual cortex is beyond the scope of this study, a
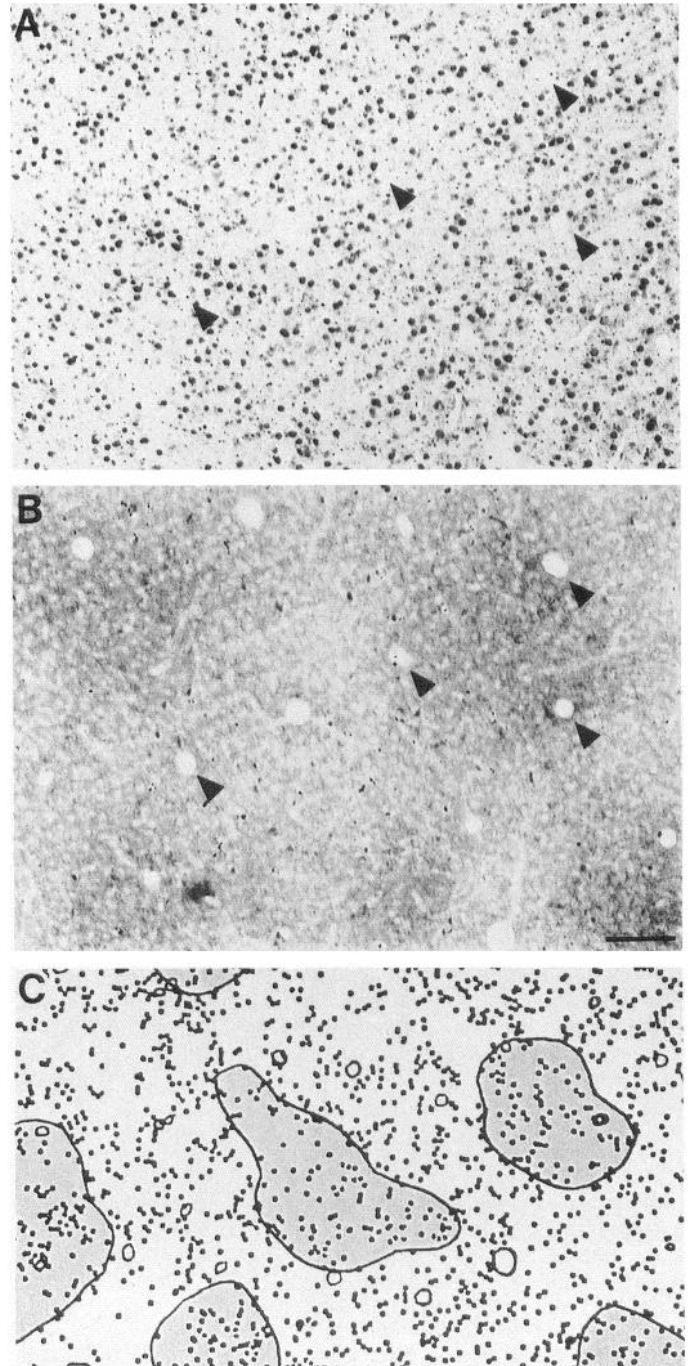


*Figure 4.* Pairs of photomicrographs of adjacent sections through layer III of monkey V1 labeled immunocytochemically for NMDAR1 (*A*) or histochemically for cytochrome oxidase activity (*B*), and a map (*C*) in which a different set of sections were overlain. Labeled somata were present in both cytochrome oxidase–rich puffs and in the intervening cytochrome oxidase–poor regions, with no overt parcellation to either compartment. *Arrowheads* in *A* and *B* denote blood vessels common to both sections. Scale bar, 100 $\mu$m.

←

*Figure 3.* NMDAR1 immunoreactivity in monkey V1. *A,* Map showing laminar distribution of labeled somata. *B* and *C,* Photomicrographs of sections cut in the frontal plane through layers I–III (*B*) or cut obliquely through layers IVC$\beta$–VI (*C*). As in other areas, labeled apical dendrites could be followed from pyramidal cell somata in layer II into layer I (*arrowheads in B*), forming a plexus there. Small, faintly labeled somata were also present in layer I (*open arrow in B*). In obliquely cut sections through deep layers, small clusters of cut dendrites were observed in layers V and VI (*arrowheads in C*). Scale bar, 50 $\mu$m.

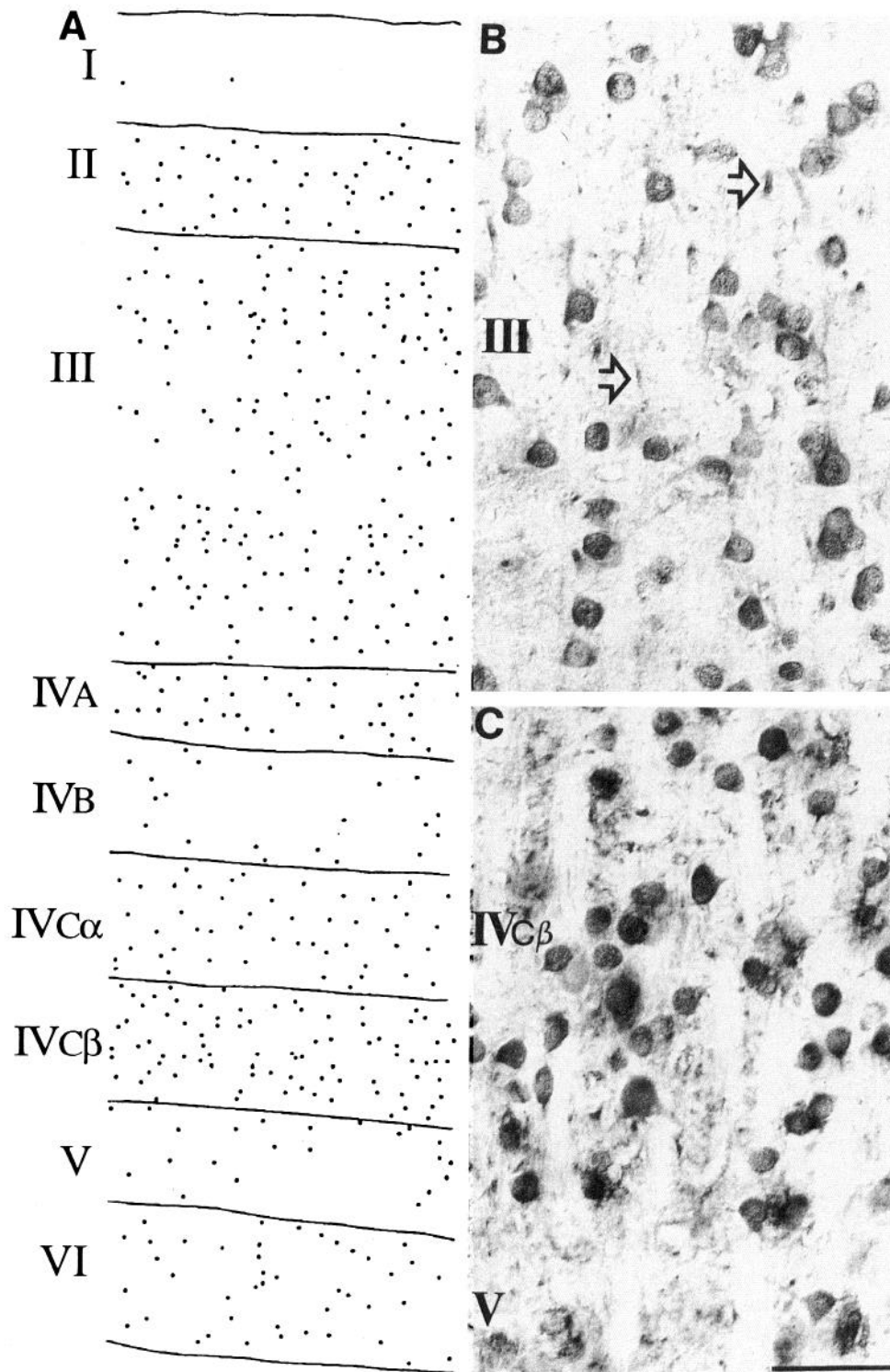*Figure 5.* NMDAR1 immunoreactivity in human V1. *A*, Map showing laminar distribution of labeled somata. *B* and *C*, Photomicrographs through indicated layers showing cellular staining patterns. Prominent, labeled apical dendrites were less frequently observed in comparison with monkey cortex, although in the neuropil were some labeled segments of thick fibers (*open arrows in B*). Layer IVCβ was densely packed with small, round stained somata, similar to the monkey. Scale bar, 50 μm.

large number of cells in all cell-dense layers of each of the areas examined appeared immunolabeled, similar to the pattern detailed previously for monkey prefrontal cortex (Vickers et al., 1993). In each area, all GluR2/3-immunoreactive cells were also immunoreactive for NMDAR1 subunits (Table 2, Fig. 6*A,B*). Although the converse relationship was not specifically examined, qualitative observations suggest that in sensory-motor cortex, the two populations were mostly identical. In visual cortex, a substantial number of NMDAR1-immunoreactive cells (mostly in middle layers) were found that were not GluR2/3 immunoreactive.

The percentage of GluR5/6/7-immunoreactive cells that were NMDAR1 immunoreactive was determined indirectly, through colocalization studies with the polyclonal antisera to GluR2/3. The percentage of cells GluR5/6/7 immunoreactive that colocalized GluR2/3 subunits was found to be 100% in each of the
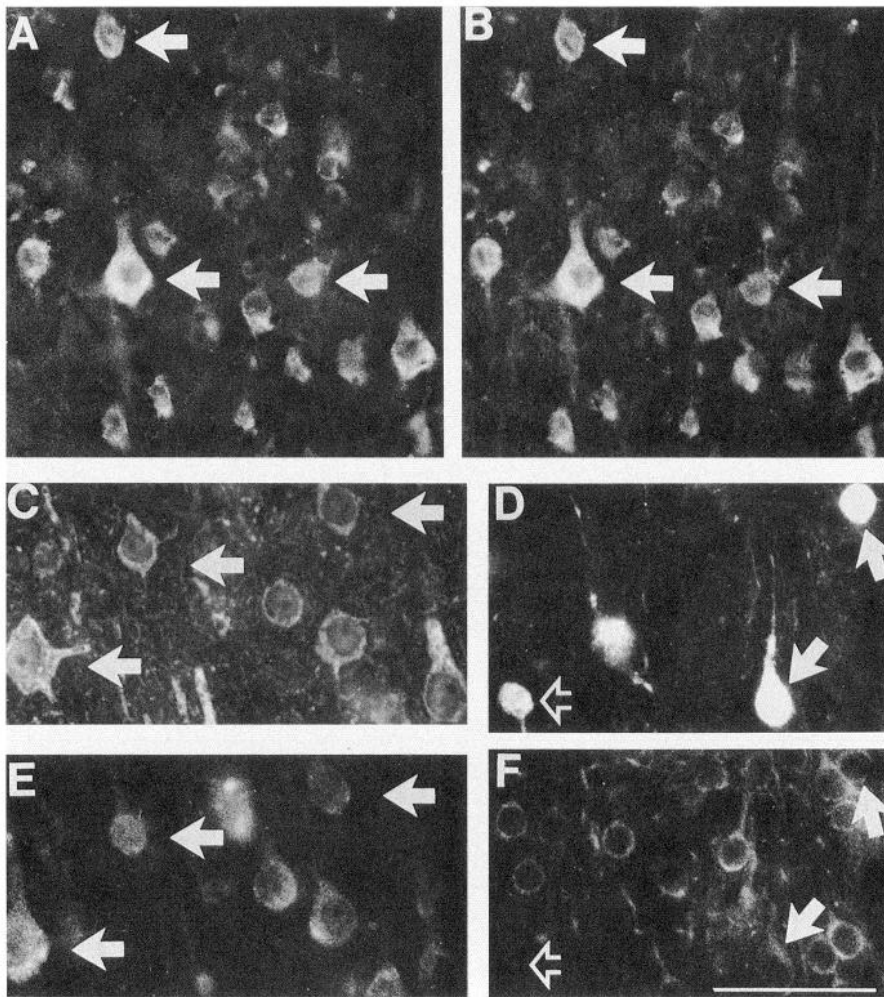
*Figure 6.* Pairs of fluorescence photomicrographs taken from single sections of monkey cortex showing colocalized combinations of NMDAR1, non-NMDA subunits, and calcium-binding proteins. *A* and *B*, Section through layer III of area 1 showing cells (*arrows*) immunoreactive for both GluR2/3 (*A*) and NMDAR1 (*B*). *C* and *E*, Section through layer III of M1 showing cells (*arrows*) immunoreactive for both GluR5/6/7 (*C*) and GluR2/3 (*E*). *D* and *F*, Section showing cells in layer IVCβ of V1 immunofluorescently labeled for parvalbumin (*solid arrows; D*), all of which except one (*open arrow*) are also NMDAR1 immunoreactive (*F*). Scale bar, 50 μm.

primary sensory and motor areas examined (Table 2, Fig. 6*C,E*), a figure identical to that found in monkey prefrontal cortex (Vickers et al., 1993). The converse relationship was not quantitatively examined, although in each area, qualitative observations suggest that GluR2/3-containing cells formed the larger population, especially in V1, where there are relatively fewer GluR5/6/7-immunoreactive cells in comparison to other areas (see Huntley et al., 1993). In any case, it follows that since GluR5/6/7-immunoreactive cells contain GluR2/3 subunits, and the latter cells contain NMDAR1 subunits, then GluR5/6/7-immunoreactive cells must also possess NMDAR1 subunits.

NMDAR1 immunoreactivity in the cells labeled by calcium-binding protein immunoreactivity was often faint, and generally did not extend very far into the proximal dendrites. The vast majority of PV-immunoreactive somata in each of the areas were NMDAR1 immunopositive (Table 2, Fig. 6*D,F*). In contrast, only a minority of the CR-immunoreactive cells were NMDAR1 immunoreactive (Table 2). In both cases, there did not appear to be any overt correlation between the PV- or CR-labeled cells *not* NMDAR1 immunolabeled and their laminar location.

## Electron microscopy

NMDAR1 immunoreactivity was present throughout the cytoplasm of both dendrites (Fig. 7*A–D*) and cell somata (Fig. 7*E*), and was only very rarely localized to presynaptic axon terminals. In many cases, especially in dendrites, the clumped and dense nature of the precipitate obscured the underlying organelles.

**Table 2. Colocalization of NMDAR1 subunits with non-NMDA subunits and calcium-binding proteins**

|  | M1 | S1[a] | V1 |
|---|---|---|---|
| PV vs NMDAR1 | 89.9 ± 0.3 | 87.7 ± 1.2 | 83.4 ± 1.7 |
| CR vs NMDAR1 | 6.2 ± 0.7 | 6.8 ± 0.4 | 8.5 ± 0.5 |
| GluR2/3 vs NMDAR1 | 100 | 100 | 100 |
| GluR5/6/7 vs GluR2/3 | 100 | 100 | 100 |

Data are given as mean percentages ± SD. See Materials and Methods for details.

[a] Data from S1 were taken through area 3b.
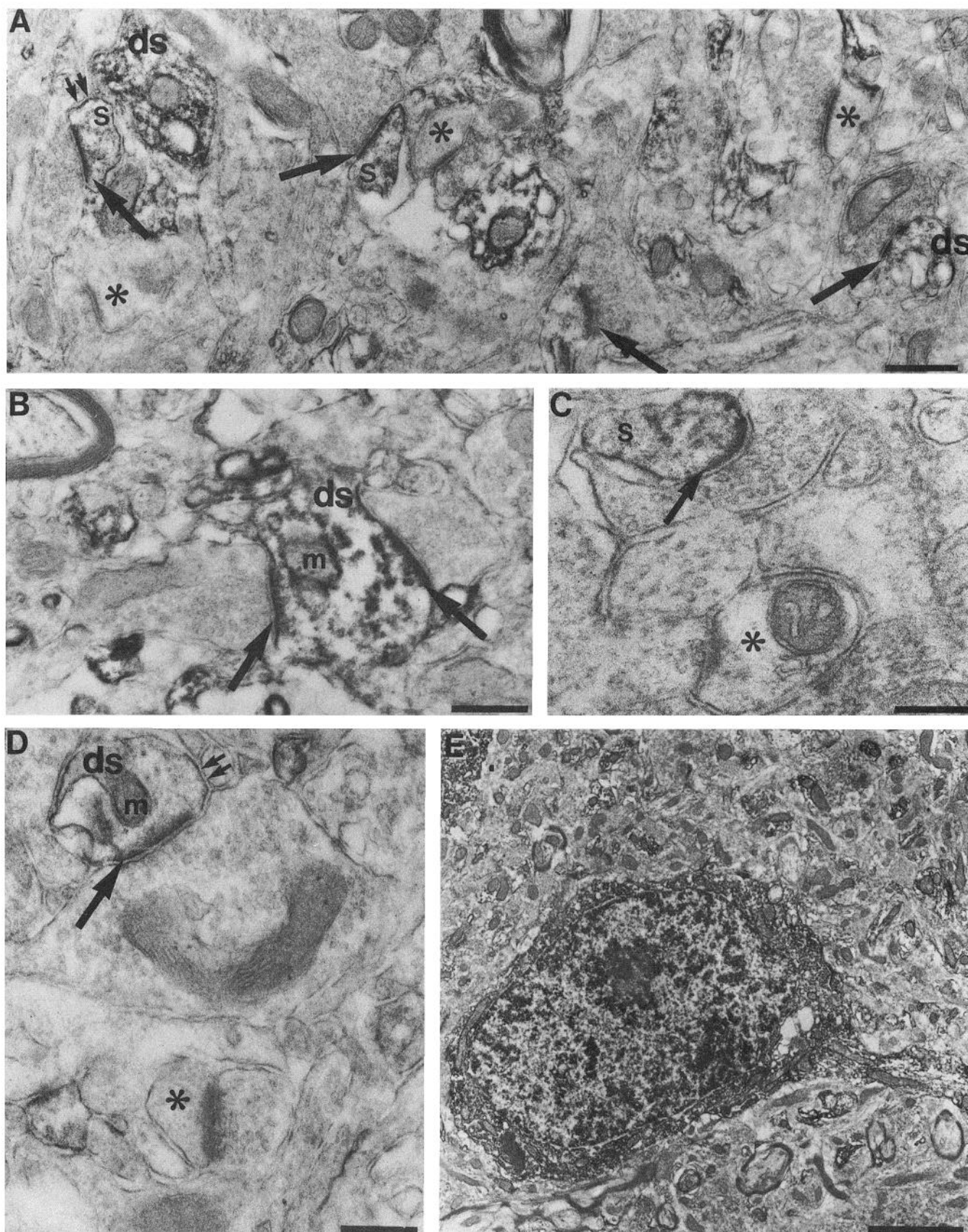
*Figure 7.* Ultrastructural localization of NMDAR1 immunoreactivity in monkey cortex shown in electron photomicrographs of sections taken through superficial layers of M1 (*A*) or V1 (*D*) and through layer IV of area 3b (*B*) or IVC$\beta$ of V1 (*C, E*). Numerous, intensely labeled asymmetrical postsynaptic densities were present in all layers examined (*single arrows, A–D*), which were located on both dendritic shafts (*ds*) and spines (*s*). Many unlabeled asymmetrical synapses were also present in all layers (*asterisks, A–D*). Immunoreactivity often lined the membranes of unstained

Occasionally, segments of the plasma membrane of dendrites were immunolabeled (double arrows, Fig. 7A,D). Within pyramidal cell somata, immunoprecipitate was often associated with stacks of rough endoplasmic reticulum, and could sometimes be seen lining the outer membranes of otherwise unstained mitochondria, as well. In layer IVC of V1, the majority of the interneuronal cell somata were labeled (Fig. 7E), and many possessed ultrastructural features that have been described as characteristic of spiny stellate cells (e.g., Lund, 1984; Saint Marie and Peters, 1985), including a large and mostly circular nucleus, a high nucleus:cytoplasm volume ratio, and minimal cytoplasm with fewer organelles.

Labeled synapses were identified by intense immunolabeling of postsynaptic densities, which were asymmetrical and in apposition to presynaptic terminals containing round vesicles (single arrows, Fig. 7A–D), as well as by the presence of reaction product within the surrounding cytoplasm. The synaptic clefts did not appear to be labeled. The postsynaptic elements in each of the layers examined were both small dendritic shafts and dendritic spines (Fig. 7A–D), although many shafts and spines were unlabeled (asterisks, Fig. 7A–D). Across each of the three areas examined, the percentages of the asymmetrical synapses that were NMDAR1 immunoreactive were determined in supragranular layers, layers IV (area 3b) or IVC$\beta$ (V1), and deep layers (Table 3). The percentages of NMDAR1-immunoreactive synapses were similar between superficial and deep layers in M1, but exhibited more pronounced laminar variations in the primary sensory areas (Table 3), with a particular prevalence for superficial layers in V1 and layer IV in area 3b. No attempt was made to determine the proportion of labeled postsynaptic elements that were shafts or spines.

## Discussion

Immunocytochemical methods were used to localize NMDAR1 subunit proteins in primate sensory-motor and visual cortex, and to examine, quantitatively, features of their synaptic organization and codistribution with non-NMDA ionotropic glutamate receptor subunits and calcium-binding proteins. The principal conclusions that emerge from the present study are (1) cortical cells that possess NMDA receptors constitute a morphologically, functionally, and neurochemically diverse population, and are well represented in all layers of the primary somatic sensory, motor, and visual cortex; (2) in each of the areas examined, a significant proportion (20–46%) of the asymmetrical synapses found in superficial layers, layer IV, and deep layers were NMDAR1 immunoreactive, although the proportions of immunopositive synapses varied by lamina in S1 and V1 while in M1, the proportions of immunopositive synapses were more similar between deep and superficial layers; (3) the laminar and synaptic organization of NMDAR1 subunits suggests that NMDA receptors can potentially mediate the activity of a broad set of excitatory circuits of putative local and extrinsic origin, such as thalamocortical afferents, and may underlie the kinds of plasticity in motor and sensory maps that have been demonstrated in these areas.

Table 3. Percentages of NMDAR1-immunoreactive synapses in M1, S1, and V1

| | M1 | S1[a] | V1 |
|---|---|---|---|
| II/III | 46.0 (52/113) | 26.4 (83/314) | 44.3 (144/325) |
| IV[b] | — | 45.6 (68/149) | 34.5 (91/264) |
| V/VI | 40.8 (53/130) | 37.4 (92/246) | 19.2 (53/276) |

Values represent percentages of total asymmetrical synapses that were NMDAR1 immunoreactive (raw numbers in parentheses) counted from randomly chosen fields through the indicated layer(s) and areas.
[a] Data from S1 were taken through area 3b.
[b] IVC$\beta$ in V1.

### Cell types exhibiting NMDAR1 immunoreactivity in neocortex

NMDAR1 immunoreactivity was localized to cells of each of the fundamental neuronal classes present in cerebral cortex, including pyramidal cells, nonpyramidal GABAergic inhibitory interneurons—identified by their immunoreactivity for certain calcium-binding proteins (Celio, 1986; Hendry et al., 1989)—and nonpyramidal spiny stellate cells. The identification of labeled spiny stellate cells was indirect, since no neurochemical markers exist that exclusively identify this cell population. However, the neuronal composition of layer IVC in monkey area V1 consists of only two cell types, approximately 85–95% of which are spiny stellate cells (Lund, 1973; Tigges et al., 1977), while the remaining number are GABAergic interneurons (Hendrickson et al., 1981; Fitzpatrick et al., 1987; Hendry et al., 1987), which can be identified by their PV immunoreactivity (Hendry et al., 1989; van Brederode et al., 1990). While many PV-immunoreactive cells in layer IV of monkey area V1 were also NMDAR1 immunoreactive, the additional numbers of NMDAR1-immunolabeled cells present suggest that spiny stellate cells were also immunolabeled. Moreover, many of the labeled somata in layer IVC of V1 had ultrastructural features characteristic of spiny stellate cells (Lund, 1984; Saint Marie and Peters, 1985). The presence of labeled spiny stellate cells (or "star pyramids"; Lorente de Nó, 1938) in S1 was less certain, since layer IV contains a more heterogeneous population of cells than does layer IV in V1 (Jones, 1975). The morphological and functional diversity represented by the cortical neurons possessing NMDAR1 immunoreactivity is consistent with the widespread role NMDA receptors are thought to play in a variety of neuronal functions (Cotman et al., 1988; Constantine-Paton et al., 1990). In addition, the patterns of colocalization of NMDAR1 subunits with non-NMDA ionotropic glutamate receptor subunits and calcium-binding proteins suggest that neurochemically heterogeneous subpopulations of NMDAR1-immunoreactive cells are present in neocortex.

### Neurochemically defined subpopulations of NMDAR1-immunoreactive cells

Across each of the areas examined, 100% of the cells immunoreactive for AMPA/kainate receptor subunits GluR2/3 were also NMDAR1 immunoreactive. These data suggest that both

←

mitochondria (m, B and D), and occasionally the plasma membrane along segments of dendrites (double arrows, A and D) in addition to the more diffuse dendritoplasmic labeling. The somata of many interneurons in layer IVC$\beta$ were also labeled (E). Scale bars: A, 0.5 $\mu$m; B and D, 0.3 $\mu$m; C, 0.2 $\mu$m; E, 2 $\mu$m.

NMDA and non-NMDA ionotropic glutamate receptors may be operational in a large majority of neocortical cells, which is supported by studies showing that evoked excitatory activity of many cells is dependent on both NMDA and non-NMDA receptor–mediated components (reviewed in Ascher and Nowak, 1987). Although the present study did not specifically address the issue of whether, at the ultrastructural level, NMDA and non-NMDA receptors are present at the same synapses, synaptic colocalization is likely, since physiological studies suggest that NMDA and non-NMDA receptors are concentrated at the same synapses in cultured neurons from rat hippocampus (Bekkers and Stevens, 1989) and visual cortex (Jones and Baughman, 1991). The immunolabeled plasma membranes found along some dendritic segments may reflect extrasynaptic receptors, although the density of these is thought to be low (Jones and Baughman, 1991). Regardless, the presence and subunit composition of colocalized NMDA and non-NMDA receptors may be cell and circuit specific, since discrete synaptic currents in cultured hippocampal cells (Bekkers and Stevens, 1989) or EPSPs generated from cortical sensory-motor cells (Thomson, 1986) can be purely NMDA receptor dependent, purely non-NMDA receptor dependent, or dependent on both receptor classes. While it is probably unlikely that NMDAR1 subunits and any of the non-NMDA receptor subunits assemble together to form native glutamate receptor ion channels (Brose et al., 1993), the present and previous colocalization data suggest which combinations of individual NMDA and non-NMDA receptor subunits coexist in single cells. Quantitative studies in monkey prefrontal cortex have shown that 100% of the GluR5/6/7-immunoreactive cells are also GluR2/3 immunoreactive, with the former population representing a subset of the latter population (Vickers et al., 1993). This pattern is similar in monkey sensory-motor and visual cortex (Table 2). Although colocalization of GluR5/6/7 subunits and NMDAR1 subunits was not directly examined in the present study, the complete colocalization of GluR2/3 with NMDAR1 suggests that all cells in sensory-motor and visual cortex that were GluR5/6/7 immunopositive would also be NMDAR1 immunopositive, a conclusion similar to one determined from the more direct double-labeling studies of monkey hippocampus (Siegel et al., 1994). Thus, there would seem to be one cell population in neocortex that possesses at least NMDAR1, GluR2/3, and GluR5/6/7 subunits, while a separate population possesses NMDAR1 and GluR2/3 subunits, but not GluR5/6/7 subunits. The relative proportions of each of these cell populations are likely to vary regionally, since the density of GluR5/6/7-immunoreactive cells is much lower in primary somatic sensory and visual cortex in comparison with motor and higher-order association cortex (Huntley et al., 1993).

These data indicate that subpopulations of NMDAR1-immunoreactive neurons exist in monkey cortex that can be defined in terms of differential expression of non-NMDA receptor subunits. Although both NMDA and non-NMDA receptors have been linked to the vulnerability to cell death associated with excitotoxicity, neurodegenerative disorders, and ischemia (Choi, 1988; Greenamyre and Young, 1989), the presence of NMDA receptors alone does not seem to correlate significantly with regional or cellular patterns of vulnerability (Meldrum and Garthwaite, 1991). For example, visual area V1 is one of the cortical areas most resistant to degeneration (Morrison, 1993), but NMDAR1-immunoreactive cells are present throughout this region. Therefore, the individual *combinations* of NMDA and non-NMDA glutamate receptor subunits in cortical neurons and the regional patterns in which neurons with different combinations are distributed may ultimately reflect more accurately the degree to which different classes of neurons exhibit vulnerability to glutamate-related cell death (see also Vickers et al., 1993).

The role of NMDA receptors in the function of GABAergic neurons is unclear. Physiological studies of rat motor cortical slices have shown that stimulation of the corpus callosum produces, indirectly, both GABA$_B$ receptor–mediated IPSPs, which could be suppressed by blocking NMDA receptors, and GABA$_A$ receptor–mediated IPSPs, which could be suppressed by blocking non-NMDA receptors (Kawaguchi, 1992). These data suggest a differential involvement of NMDA and non-NMDA receptors in mediating the excitatory inputs to GABAergic neurons. It has been suggested in studies of neocortical slice preparations from rat and cat that postsynaptic GABA$_B$ receptor–mediated IPSPs are most prominent at, or near, cell somata (Connors et al., 1988). This would imply that GABAergic cells whose axons target somata or nearby regions may have a greater representation of NMDA receptors than ones whose axons target more distal dendrites. In this regard, it may be significant that the majority ($\sim$80–90%) of the PV-immunoreactive cells in sensory-motor and visual cortex were NMDAR1 immunoreactive, while only $\sim$6–9% of the CR-immunoreactive cells were. PV-immunoreactive cells include basket and chandelier cells (DeFelipe et al., 1989; Hendry et al., 1989; Lewis and Lund, 1990; Williams et al., 1992), subtypes of GABAergic neurons whose axons target primarily cell somata and axon initial segments, respectively (Jones and Hendry, 1984; Peters, 1984). Moreover, a recent study showed that excitation of basket-like neurons in entorhinal cortex was mediated largely by NMDA receptors (Jones and Bühl, 1993). In rats, the axons of CR-immunoreactive cells target distal dendrites (Luth et al., 1993), consistent with previous suggestions that both calbindin and calretinin label a population that includes double-bouquet cells (DeFelipe et al., 1990; DeFelipe and Jones, 1992), a class of GABAergic cells whose axons target more distal dendrites (Somogyi and Cowey, 1984). Whether calbindin-immunoreactive cells are NMDAR1 immunoreactive is not known. Nevertheless, the data suggest that NMDA receptors may play a selective role in mediating the activity of GABA cells with discrete synaptic targets, thereby modulating specific aspects of inhibitory cortical circuitry.

*NMDA receptors in human visual cortex*

The inability to achieve adequate immunolabeling in human postmortem material restricted the number of human cases that could be examined, since acquisition of area 17 biopsy material is difficult. Thus, given that only a single case was examined, the data should be interpreted with caution, and conclusions regarded as tentative.

NMDAR1-immunoreactive cells in human V1 were distributed in a laminar pattern largely similar to the distribution of NMDA receptor binding sites in human V1 revealed by autoradiographic methods (Jansen et al., 1989; Albin et al., 1991), which, collectively, supports a role for NMDA receptors as a component of the excitatory circuitry of human visual cortex. It remains to be determined, however, precisely where, at the synaptic level, NMDA receptors are operative. Given that the overall laminar distribution of NMDAR1-immunoreactive cells in human V1 was mostly similar to that in monkey V1, the synaptic organization may also be similar to that in monkeys.

The major difference in the patterns of immunoreactivity at the light microscopic level between the two primate species was diminished fine-caliber fiber staining in the neuropil of layer I and other layers in human V1, which could be due to differences in tissue processing (biopsy vs perfused). The distribution of immunoreactivities for non-NMDA subunits (GluR2/3 and GluR5/6/7) in several neocortical areas in human (J. C. Vickers et al., unpublished observations) also matches very closely that in monkeys (Huntley et al., 1993; Vickers et al., 1993), which may indicate a basic similarity between the cortices of monkeys and humans in the functional organization of excitatory amino acid receptors and the circuits in which they participate.

*Laminar and synaptic organization of NMDAR1 subunits: role of NMDA receptors in sensory-motor and visual function*

The laminar distribution of NMDAR1 immunoreactivity in monkey neocortex was largely consistent with, but not identical to, the reported distribution of autoradiographically localized NMDA receptor binding sites in nonhuman primate neocortex (Geddes et al., 1989). The variations between the patterns revealed by the two methods could reflect the presence of additional NMDA receptor subunits (e.g., NMDAR2, A–D), which, when combined with NMDAR1 subunits, yield receptor complexes with distinct pharmacological properties (Nakanishi, 1992). In rats, NMDAR2 subunit mRNAs show a more selective distribution than NMDAR1 subunit mRNA (Nakanishi, 1992), although the distribution of these subunits in monkey cortex is unknown. It is also likely that much of the cytoplasmically localized NMDAR1 immunoreactivity, including, for example, that surrounding the outer mitochondrial membranes and other organelles, does not reflect functional receptors, but rather represents epitope sites associated with receptor assembly, degradation, or transport. Similar patterns of intracellular receptor localization are also evident in immunoelectron microscopic studies localizing NMDAR1 subunits in hippocampus (Siegel et al., 1994) and subunits of the kainate and AMPA/kainate receptor classes in neocortex and hippocampus (Petralia and Wenthold, 1992; Good et al., 1993; Huntley et al., 1993), which may indicate that large cytoplasmic reserves of subunits of each of the three major classes of ionotropic glutamate receptors enable rapid shifts in the composition of local subunit assemblies, as metabolic or functional demands require.

NMDAR1-immunoreactive synapses were distributed in superficial and deep layers, as well as in layer IV, indicating that NMDA receptors are at least anatomically positioned to mediate a large share of the activity of the numerous excitatory pathways of extrinsic and intracortical origin. Physiological studies in cortical slices have shown that NMDA receptors contribute to the generation of EPSPs following the stimulation of callosal and corticocortical pathways as well as of horizontally directed, local pyramidal cell axon collaterals (Thomson, 1986; Jones and Baughman, 1988; Shirokawa et al., 1989; Sutor and Hablitz, 1989; Nishigori et al., 1990; Larson-Prior et al., 1991; Kawaguchi, 1992; Nicoll et al., 1992; but see Hirsch and Gilbert, 1991). In the sensory-motor and visual areas of monkeys, such projections mainly arise from and terminate in supragranular layers (Valverde, 1985; Jones, 1986), targeting predominantly dendritic spines, but also dendritic shafts (Colonnier, 1968; Jones and Powell, 1970; Winfield et al., 1981; Feldman, 1984; Kisvarday et al., 1986; McGuire et al., 1991; White and Czeiger, 1991). These data are consistent with the present anatomical findings, in which a significant proportion (~25–45%) of the

supragranular asymmetrical synapses in sensory-motor and visual cortex were NMDAR1 immunopositive, localized to both dendritic spines and shafts. While many of the postsynaptic elements in superficial layers were likely to originate from the numerous labeled cell somata in layers II and III, the small caliber of some of the labeled postsynaptic shafts may reflect, in part, the distal apical dendrites that arise from the many labeled pyramidal cells present in deeper layers. In addition, a large number of the ascending apical dendrites of pyramidal cells form their terminal dendritic arbors in the inner half of layer I (Feldman, 1984). There is evidence in rats that NMDA receptors can mediate the activity of the projections to cortex from certain thalamic intralaminar nuclei (Fox and Armstrong-James, 1986), which may reflect the plexus of NMDAR1-immunolabeled fibers in the inner half of layer I. In the monkey cortical areas examined, projections from the intralaminar nuclei terminate mostly in layer I (Jones, 1985). In layers II and III, NMDA receptors appear to play a dominant role in the generation of naturally elicited, sensorially driven activity in rat barrel cortex (Armstrong-James et al., 1993) and in cat and kitten visual cortex (Tsumoto et al., 1987; Fox et al., 1989; Miller et al., 1989) These data indicate that in primates, NMDA receptors in layers II/III probably also contribute substantially to the transmission of visual, somatic sensory, or motor information (Shima and Tanji, 1993), possibly in the context of experience-dependent synaptic plasticity of the kind thought to underlie learning and memory. For example, some forms of long-term potentiation (LTP), a type of use-dependent synaptic modification that has been linked to such functions (Bliss and Collingridge, 1993), are dependent on NMDA receptor activation (Collingridge and Singer, 1990), and have been demonstrated in the supragranular layers of monkey motor cortex (Iriki et al., 1989, 1991) and in those of rat and kitten visual cortex (Artola and Singer, 1987; Komatsu et al., 1988; Kirkwood et al., 1993). It remains to be determined whether, at a finer level, NMDA receptors in cortex are selectively engaged by excitatory afferents bearing certain components of sensory information, or contribute preferentially to the establishment of particular receptive field properties. In monkey V1, the receptive field properties of neurons that lie within the supragranular cytochrome oxidase puffs vary substantially in comparison to those that lie between the puffs (Livingstone and Hubel, 1984), due largely to the anatomical segregation of thalamic and intracortical pathways conveying functionally distinct components of visual information (Livingstone and Hubel, 1982; DeYoe and Van Essen, 1988). The lack of any apparent differential parcellation of NMDAR1-immunoreactive cells to cytochrome oxidase–rich or –poor regions in V1 may indicate that sensory information processing mediated by NMDA receptors in neocortex is not necessarily restricted to particular receptive field properties or pathways (see also Fox et al., 1989).

In contrast to the close association between NMDA receptor localization and functional expression in superficial layers, the role of NMDA receptors in layers IV–VI in a functional context is more ambiguous. For example, iontophoresis of the NMDA receptor antagonist D-2-amino-5-phosphonovaleric acid (APV) onto neurons in layers IV–VI of adult cat visual cortex affects only their spontaneous activity, but has no effect on visually driven responses in these layers (Fox et al., 1989). By contrast, whisker deflection results in significant NMDA receptor activation in layer IV of rat S1 barrel cortex (Armstrong-James et al., 1993). Although these data could reflect species differences

in the organization of NMDA receptors within layer IV, they could also reflect more fundamental differences in the number, density, or organization of NMDA receptor–linked synapses across different layers, and perhaps even between different areas. This possibility is consistent with the present findings, in which the percentages of asymmetrical synapses that were NMDAR1 immunopositive varied across layers, and across areas. The percentages of NMDAR1-immunoreactive synapses in superficial and deep layers of M1 were relatively similar to each other in comparison to the more pronounced laminar differences observed in the primary sensory areas, which could be a reflection of the inherently different cellular organization of motor cortex in comparison to sensory cortex that is evident in the lack of a clear layer IV in adult M1. Since thalamocortical axons represent a major afferent system targeting layer III in motor cortex and mainly layers III–IV in primary sensory areas (Hubel and Wiesel, 1972; Jones, 1986), the observation that 35–45% of the asymmetrical synapses in the principal thalamorecipient layers were NMDAR1 immunopositive suggests an important role for NMDA receptors in the mediation of thalamocortical activity or other excitatory afferents that target these layers, such as those from the claustrum, other cortical areas, or local intralaminar sources (e.g., Riche and Lanoir, 1978; Lund, 1984; Jones, 1986). On the other hand, since local axon collaterals of pyramidal cells and spiny stellate cells provide the majority of the excitatory synapses in cortex in comparison to those provided by axons from the thalamus or other extrinsic sources (White, 1989), the majority of NMDA-immunoreactive synapses may reflect mostly local circuits. Regardless, the origin of the presynaptic components of the NMDAR1-immunoreactive synapses in layer IV and in deeper layers, and the precise functional role NMDA receptors play there remain to be determined.

While it would appear that NMDA receptors in granular and infragranular layers are at least anatomically poised to mediate the activity of a variety of excitatory inputs, it may be the case that under most conditions, they are functionally quiescent. NMDA receptor–mediated activity is prominent in the monosynaptic thalamocortical response in slices of immature cortex (Agmon and O'Dowd, 1992), but is not evident in the earliest monosynaptic thalamocortical responses in adult cortex (Fox et al., 1989; Larson-Prior et al., 1991; Armstrong-James et al., 1993). While these data may be accounted for by developmentally regulated changes in the number or location of functional NMDA receptors over time in a manner akin to other neurotransmitter-receptor systems (Parnavelas et al., 1988), the significant numbers of NMDAR1-immunoreactive cells and synapses present in layers IV–VI of adult monkey cortex suggest that other modulatory influences may exist that effectively inhibit NMDA receptor activation. GABAergic inhibition, for example, has a profound effect on the generation of NMDA receptor–mediated responses (Artola and Singer, 1987; Luhmann and Prince, 1990a,b; Agmon and O'Dowd, 1992) and the expression of NMDA receptor–dependent LTP (Steward et al., 1990). Thus, relative differences observed between superficial and deeper layers in the extent to which NMDA receptors are involved in the generation of sensorially driven activity may be explained, in part, by differences in the efficacy or organization of GABAergic circuits between cells of different layers or classes. Variability in the density and distribution of GABAergic synaptic contacts upon cortical pyramidal cells that project to different targets, and that occupy different layers, has been described (Fairén and Valverde, 1980; Freund et al., 1983; DeFelipe

et al., 1985; Fariñas and DeFelipe, 1991a,b). Regulation of NMDA receptor function may also occur at the synaptic level. For example, calcium/calmodulin-dependent protein kinase type II (CAM II kinase), a major component of asymmetrical postsynaptic densities (Kennedy et al., 1983; Kelly et al., 1984) and present throughout sensory-motor and visual cortex (Benson et al., 1991; Jones et al., 1994), can induce phosphorylation of the NMDA receptor channel leading to increased $Ca^{2+}$ influx (Kitamura et al., 1993). In addition, zinc can potentiate agonist-induced currents through homomeric NMDA receptors assembled from certain NMDAR1 splice variants (Hollmann et al., 1992). Taken together, the integration of these data with those of the present study may bear on recent experiments suggesting that in S1, the functional reorganization of the cortical sensory map that occurs following selective deafferentation is dependent on NMDA receptor activation (Kano et al., 1991). Since alterations in sensory input can modulate levels of GABA, its synthesizing enzyme GAD, $GABA_A$ receptors, and CAM II kinase in cortical neurons (Hendry and Jones, 1986, 1988; Hendry and Kennedy, 1986; Welker et al., 1989; Hendry et al., 1990; Benson et al., 1991), changes in GABAergic inhibition or second messenger systems could unmask previously silent NMDA receptor–mediated inputs and/or change the functional properties associated with such inputs, thus possibly representing one mechanism for the rapid activity-dependent changes that can be induced in the representational maps of sensory-motor and visual cortex (e.g., Merzenich et al., 1983, 1984; Donoghue and Sanes, 1988; Donoghue et al., 1990; Kaas et al., 1990; Nudo et al., 1990; Garraghty and Kaas, 1991; Jacobs and Donoghue, 1991; Pons et al., 1991).

# References

Agmon A, O'Dowd DK (1992) NMDA receptor-mediated currents are prominent in the thalamocortical synaptic response before maturation of inhibition. J Neurophysiol 68:345–349.

Albin RL, Sakurai SY, Makowiec RL, Higgins DS, Young AB, Penney JB (1991) Excitatory amino acid, GABA-A, and GABA-B binding sites in human striate cortex. Cereb Cortex 1:499–509.

Anantharam V, Panchal RG, Wilson A, Kolchine VV, Treistman SN, Bayley H (1992) Combinatorial RNA splicing alters the surface charge on the NMDA receptor. FEBS Lett 305:27–30.

Armstrong-James M, Welker E, Callahan CA (1993) The contribution of NMDA and non-NMDA receptors to fast and slow transmission of sensory information in the rat SI barrel cortex. J Neurosci 13:2149–2160.

Artola A, Singer W (1987) Long-term potentiation and NMDA receptors in rat visual cortex. Nature 330:649–652.

Ascher P, Nowak L (1987) Electrophysiological studies of NMDA receptors. Trends Neurosci 10:284–288.

Bekkers JM, Stevens CF (1989) NMDA and non-NMDA receptors are co-localized at individual excitatory synapses in cultured rat hippocampus. Nature 341:230–233.

Benson DL, Isackson PJ, Gall CM, Jones EG (1991) Differential effects of monocular deprivation on glutamic acid decarboxylase and type II calcium-calmodulin-dependent protein kinase gene expression in the adult monkey visual cortex. J Neurosci 11:31–47.

Bliss TVP, Collingridge GL (1993) A synaptic model of memory: long-term potentiation in the hippocampus. Nature 361:31–39.

Brodmann K (1905) Beiträge zur histolgischen Lokalisation der Grosshirnrinde: die Rindenfeldern der niederen Affen. J Psychol Neurol 4:177–226.

Brose N, Gasic GP, Rogers SW, Moran T, Morrison JH, Jahn R, Heinemann SF (1993) Immunoaffinity purification of glutamate receptors of the non-NMDA and NMDA type. Soc Neurosci Abstr 19:1356.

Celio MR (1986) Parvalbumin in most gamma-aminobutyric acid-containing neurons of the rat cerebral cortex. Science 231:995–997.

Choi DW (1988) Glutamate neurotoxicity and diseases of the nervous system. Neuron 1:623–634.

Collingridge GL, Bliss TVP (1987) NMDA receptors-their role in long-term potentiation. Trends Neurosci 10:288–293.

Collingridge GL, Singer W (1990) Excitatory amino acid receptors and synaptic plasticity. Trends Pharmacol Sci 11:290–296.

Colonnier M (1968) Synaptic patterns on different cell types in the different laminae of the cat visual cortex, an electron microscope study. Brain Res 9:268–287.

Connors BW, Malenka RC, Silva LR (1988) Two inhibitory postsynaptic potentials, and GABA_A and GABA_B receptor-mediated responses in neocortex of rat and cat. J Physiol (Lond) 406:443–468.

Constantine-Paton M, Cline HT, Debski E (1990) Patterned activity, synaptic convergence and the NMDA receptor in developing visual pathways. Annu Rev Neurosci 13:129–154.

Cotman CW, Monaghan DT, Ganong AH (1988) Excitatory amino acid neurotransmission: NMDA receptors and Hebb-type synaptic plasticity. Annu Rev Neurosci 11:61–80.

DeFelipe J, Jones EG (1992) High-resolution light and electron microscopic immunocytochemistry of colocalized GABA and calbindin D-28k in somata and double bouquet cell axons of monkey somatosensory cortex. Eur J Neurosci 4:46–60.

DeFelipe J, Hendry SHC, Jones EG, Schmechel D (1985) Variability in the terminations of GABAergic chandelier cell axons on initial segments of pyramidal cell axons in the monkey sensory-motor cortex. J Comp Neurol 231:364–384.

DeFelipe J, Hendry SHC, Jones EG (1989) Visualization of chandelier cell axons by parvalbumin immunoreactivity in monkey cerebral cortex. Proc Natl Acad Sci USA 86:2093–2097.

DeFelipe J, Hendry SHC, Hashikawa T, Molinari M, Jones EG (1990) A microcolumnar structure of monkey cerebral cortex revealed by immunocytochemical studies of double bouquet cell axons. Neuroscience 37:655–673.

DeYoe EA, Van Essen DC (1988) Concurrent processing streams in monkey visual cortex. Trends Neurosci 11:219–226.

Donoghue JP, Sanes JN (1988) Organization of adult motor cortex representation patterns following neonatal forelimb nerve injury in rats. J Neurosci 8:3221–3232.

Donoghue JP, Suner S, Sanes JN (1990) Dynamic organization of primary motor cortex output in target muscles in adult rats. II. Rapid reorganization following motor nerve lesions. Exp Brain Res 79:492–503.

Dougherty PM, Palecek J, Paleckova V, Sorkin LS, Willis WD (1992) The role of NMDA and non-NMDA excitatory amino acid receptors in the excitation of primate spinothalamic tract neurons by mechanical, chemical, thermal, and electrical stimuli. J Neurosci 12:3025–3041.

Durand GM, Gregor P, Zheng X, Bennett MVL, Uhl GR, Zukin RS (1992) Cloning of an apparent splice variant of the rat N-methyl-D-aspartate receptor NMDAR1 with altered sensitivity to polyamines and activators of protein kinase C. Proc Natl Acad Sci USA 89:9359–9363.

Evans RH, Long SK (1989) Primary afferent depolarization in the rat spinal cord is mediated by pathways utilising NMDA and non-NMDA receptors. Neurosci Lett 100:231–236.

Fairén A, Valverde F (1980) A specialized type of neuron in the visual cortex of cat. A Golgi and electron microscope study of chandelier cells. J Comp Neurol 194:761–779.

Fariñas I, DeFelipe J (1991a) Patterns of synaptic input on corticocortical and corticothalamic cells in the cat visual cortex. I. The cell body. J Comp Neurol 304:53–69.

Fariñas I, DeFelipe J (1991b) Patterns of synaptic input on corticocortical and corticothalamic cells in the cat visual cortex. II. The axon initial segment. J Comp Neurol 304:70–77.

Feldman ML (1984) Morphology of the neocortical pyramidal neuron. In: The cerebral cortex, Vol 1, Cellular components of the cerebral cortex (EG Jones, A Peters, eds), pp 123–200. New York: Plenum.

Fitzpatrick D, Lund JS, Schmechel DE, Towles AC (1987) Distribution of GABAergic neurons and axon terminals in the macaque striate cortex. J Comp Neurol 264:73–91.

Fox K, Armstrong-James M (1986) The role of the anterior intralaminar nuclei and N-methyl-D-aspartate receptors in the generation of spontaneous bursts in rat neocortical neurones. Exp Brain Res 63:505–518.

Fox K, Daw NW (1993) Do NMDA receptors have a critical function in visual cortical plasticity? Trends Neurosci 16:116–122.

Fox K, Sato H, Daw N (1989) The location and function of NMDA receptors in cat and kitten visual cortex. J Neurosci 9:2443–2454.

Freund TF, Martin KAC, Smith AD, Somogyi P (1983) Glutamate decarboxylase-immunoreactive terminals of Golgi-impregnated axoaxonic cells and of presumed basket cells in synaptic contact with pyramidal neurons of the cat's visual cortex. J Comp Neurol 221:263–278.

Garraghty PE, Kaas JH (1991) Large-scale functional reorganization in adult monkey cortex after peripheral nerve injury. Proc Natl Acad Sci USA 88:6976–6980.

Gasic GP, Hollmann M (1992) Molecular neurobiology of glutamate receptors. Annu Rev Physiol 54:507–536.

Geddes JW, Cooper SM, Cotman CW, Patel S, Meldrum BS (1989) N-methyl-D-aspartate receptors in the cortex and hippocampus of baboon (Papio anubis and Papio papio). Neuroscience 32:39–47.

Good PF, Huntley GW, Rogers SW, Heinemann SF, Morrison JH (1993) Organization and quantitative analysis of kainate receptor subunit GluR5/6/7 immunoreactivity in monkey hippocampus. Brain Res, in press.

Greenamyre JT, Young AB (1989) Excitatory amino acids and Alzheimer's disease. Neurobiol Aging 10:593–602.

Hendrickson AE, Hunt SP, Wu J-Y (1981) Immunocytochemical localization of glutamic acid decarboxylase in monkey striate cortex. Nature 292:605–607.

Hendry SHC, Jones EG (1986) Reduction in number of GABA immunostained neurons in deprived-eye dominance columns of monkey area 17. Nature 320:750–753.

Hendry SHC, Jones EG (1988) Activity dependent regulation of GABA expression in the visual cortex of adult monkeys. Neuron 1:701–712.

Hendry SHC, Kennedy MB (1986) Immunoreactivity for a calmodulin-dependent protein kinase is selectively increased in macaque striate cortex after monocular deprivation. Proc Natl Acad Sci USA 83:1536–1540.

Hendry SHC, Schwark HD, Jones EG, Yan J (1987) Numbers and proportions of GABA-immunoreactive neurons in different areas of monkey cerebral cortex. J Neurosci 7:1503–1519.

Hendry SHC, Jones EG, Emson PC, Lawson DEM, Heizmann CW, Streit P (1989) Two classes of cortical GABA neurons defined by differential calcium binding protein immunoreactivities. Exp Brain Res 76:467–472.

Hendry SHC, Fuchs J, deBlas AL, Jones EG (1990) Distribution and plasticity of immunocytochemically localized GABA_A receptors in adult monkey visual cortex. J Neurosci 10:2438–2450.

Hirsch JA, Gilbert CD (1991) Synaptic physiology of horizontal connections in the cat's visual cortex. J Neurosci 11:1800–1809.

Hollmann M, Boulter J, Maron C, Beasley L, Sullivan J, Pecht G, Heinemann S (1992) Zinc potentiates agonist-induced currents at certain splice variants of the NMDA receptor. Neuron 10:943–954.

Hubel DH, Wiesel TN (1972) Laminar and columnar distribution of geniculo-cortical fibers in the macaque monkey. J Comp Neurol 146:421–450.

Huntley GW, Rogers SW, Moran T, Janssen W, Archin N, Vickers JC, Cauley K, Heinemann SF, Morrison JH (1993) Selective distribution of kainate receptor subunit immunoreactivity in monkey neocortex revealed by a monoclonal antibody that recognizes glutamate receptor subunits GluR5/6/7. J Neurosci 13:2965–2981.

Iriki A, Pavlides C, Keller A, Asanuma H (1989) Long-term potentiation in the motor cortex. Science 245:1385–1387.

Iriki A, Pavlides C, Keller A, Asanuma H (1991) Long-term potentiation of thalamic input to the motor cortex induced by coactivation of thalamocortical and corticocortical afferents. J Neurophysiol 65:1435–1441.

Jacobs KM, Donoghue JP (1991) Reshaping the cortical motor map by unmasking latent intracortical connections. Science 251:944–945.

Jansen KLR, Faull RLM, Dragunow M (1989) Excitatory amino acid receptors in the human cerebral cortex: a quantitative autoradiographic study comparing the distributions of [3H]TCP, [3H]glycine, L-[3H]glutamate, [3H]AMPA and [3H]kainic acid binding sites. Neuroscience 32:587–607.

Jones EG (1975) Varieties and distribution of non-pyramidal cells in the somatic sensory cortex of the squirrel monkey. J Comp Neurol 160:205–268.

Jones EG (1985) The thalamus. New York: Plenum.

Jones EG (1986) Connectivity of the primate sensory-motor cortex. In: The cerebral cortex, Vol 5, Sensory-motor areas and aspects of cortical connectivity (Jones EG, Peters A, eds), pp 113–183. New York: Plenum.

Jones EG, Hendry SHC (1984) Basket cells. In: Cerebral cortex, Vol 1, Cellular components of the cerebral cortex (Peters A, Jones EG, eds), pp 309–336. New York: Plenum.

Jones EG, Powell TPS (1970) An electron microscopic study of the laminar pattern and mode of termination of afferent fibre pathways in the somatic sensory cortex of the cat. Philos Trans R Soc Lond [Biol] 257:45–62.

Jones EG, Huntley GW, Benson DL (1994) Alpha calcium/calmodulin dependent protein kinase II selectively expressed in a subpopulation of excitatory neurons in monkey sensory-motor cortex: comparison with GAD-67 expression. J Neurosci 14:611–629.

Jones KA, Baughman RW (1988) NMDA- and non-NMDA-receptor components of excitatory synaptic potentials recorded from cells in layer V of rat visual cortex. J Neurosci 8:3522–3534.

Jones KA, Baughman RW (1991) Both NMDA and non-NMDA sub-types of glutamate receptors are concentrated at synapses on cerebral cortical neurons in culture. Neuron 7:593–603.

Jones RSG, Bühl EH (1993) Basket-like interneurones in layer II of the entorhinal cortex exhibit a powerful NMDA-mediated synaptic excitation. Neurosci Lett 149:35–39.

Kaas JH, Krubitzer LA, Chino YM, Langston AL, Polley EH, Blair N (1990) Reorganization of retinotopic cortical maps in adult mammals after lesions of the retina. Science 248:229–231.

Kano M, Iino K, Kano M (1991) Functional reorganization of adult cat somatosensory cortex is dependent on NMDA receptors. Neuroreport 2:77–80.

Kawaguchi Y (1992) Receptor subtypes involved in callosally-induced postsynaptic potentials in rat frontal agranular cortex in vitro. Exp Brain Res 88:33–40.

Kelly PT, McGuiness TL, Greengard P (1984) Evidence that the major postsynaptic density protein is a component of a $Ca^{2+}$/calmodulin dependent protein kinase. Proc Natl Acad Sci USA 81:945–949.

Kennedy MB, Bennett MK, Erondu NE (1983) Biochemical and immunochemical evidence that the "major postsynaptic density protein" is a subunit of a calmodulin-dependent protein kinase. Proc Natl Acad Sci USA 80:7357–7361.

Kirkwood A, Dudek SM, Gold JT, Aizenman CD, Bear MF (1993) Common forms of synaptic plasticity in the hippocampus and neocortex in vitro. Science 260:1518–1521.

Kisvarday ZF, Martin KAC, Freund TF, Magloczky Z, Whitteridge D, Somogyi P (1986) Synaptic targets of HRP-filled layer III pyramidal cells in the cat striate cortex. Exp Brain Res 64:541–552.

Kitamura Y, Miyazaki A, Yamanaka Y, Nomura Y (1993) Stimulatory effects of protein kinase C and calmodulin kinase II on N-methyl-D-aspartate receptor/channels in the postsynaptic density of rat brain. J Neurochem 61:100–109.

Kleinschmidt A, Bear MF, Singer W (1987) Blockade of "NMDA" receptors disrupts experience-dependent plasticity of kitten striate cortex. Science 238:355–238.

Komatsu Y, Fujii K, Maeda J, Sakaguchi H, Toyama K (1988) Long-term potentiation of synaptic transmission in kitten visual cortex. J Neurophysiol 59:124–141.

Kutsuwada T, Kashiwabuchi N, Mori H, Sakimura K, Kushiya E, Araki K, Meguro H, Masaki H, Kumanishi T, Arakawa M, Mishina M (1992) Molecular diversity of the NMDA receptor channel. Nature 358:36–41.

Larson-Prior LJ, Ulinski PS, Slater NT (1991) Excitatory amino acid receptor-mediated transmission in geniculocortical and intracortical pathways within visual cortex. J Neurophysiol 66:293–306.

Lewis DA, Lund JS (1990) Heterogeneity of chandelier neurons in monkey neocortex: corticotropin-releasing factor- and parvalbumin-immunoreactive populations. J Comp Neurol 293:599–615.

Livingstone MS, Hubel DH (1982) Thalamic inputs to cytochrome oxidase-rich regions in monkey visual cortex. Proc Natl Acad Sci USA 79:6098–6101.

Livingstone MS, Hubel DH (1984) Anatomy and physiology of a color system in the primate visual cortex. J Neurosci 4:309–356.

Lorente de Nó R (1938) Cerebral cortex: architecture, intracortical connections, motor projections. In: Physiology of the nervous system, 2d ed (Fulton JF, ed), pp 288–313. London: Oxford UP.

Luhmann HJ, Prince DA (1990a) Control of NMDA receptor-me-diated activity by GABAergic mechanisms in mature and developing rat neocortex. Dev Brain Res 54:287–290.

Luhmann HJ, Prince DA (1990b) Transient expression of polysynaptic NMDA receptor-mediated activity during neocortical development. Neurosci Lett 111:109–115.

Lund JS (1973) Organization of neurons in the visual cortex, area 17, of the monkey (Macaca mulatta). J Comp Neurol 147:455–496.

Lund JS (1984) Spiny stellate neurons. In: Cerebral cortex, Vol 1, Cellular components of the cerebral cortex (Peters A, Jones EG, eds), pp 255–308. New York: Plenum.

Luth H-J, Blümke I, Winkelmann E, Celio MR (1993) The calcium-binding protein calretinin is localized in a subset of interneurons in the rat cerebral cortex: a light and electron immunohistochemical study. J Hirnforsch 34:93–103.

MacDermott AB, Dale N (1987) Receptors, ion channels and synaptic potentials underlying the integrative actions of excitatory amino acids. Trends Neurosci 10:280–284.

Martin LJ, Blackstone CD, Levey AI, Huganir RL, Price DL (1993) AMPA receptor subunits are differentially distributed in rat brains. Neuroscience 53:327–358.

Mayer ML, Westbrook GL, Guthrie PB (1984) Voltage-dependent block by $Mg^{2+}$ of NMDA responses in spinal cord neurones. Nature 309:261–263.

McGuire BA, Gilbert CD, Rivlin PK, Wiesel TN (1991) Targets of horizontal connections in macaque primary visual cortex. J Comp Neurol 305:370–392.

Meguro H, Mori H, Araki K, Kushiya E, Kutsuwada T, Yamazaki M, Kumanishi T, Arakawa M, Sakimura K, Mishina M (1992) Functional characterization of a heteromeric NMDA receptor channel expressed from cloned cDNAs. Nature 357:70–74.

Meldrum B, Garthwaite J (1991) Excitatory amino acid neurotoxicity and neurodegenerative disease. Trends Pharmacol Sci 11:54–61.

Merzenich MM, Kaas JH, Wall J, Nelson RJ, Sur M, Felleman D (1983) Topographic reorganization of somatosensory cortical areas 3b and 1 in adult monkeys following restricted deafferentation. Neuroscience 8:33–56.

Merzenich MM, Nelson RJ, Stryker MP, Cynader M, Schoppman A, Zook JM (1984) Somatosensory cortical map changes following digit amputation in adult monkeys. J Comp Neurol 224:591–605.

Miller KD, Chapman B, Stryker MP (1989) Visual responses in adult cat visual cortex depend on N-methyl-D-aspartate receptors. Proc Natl Acad Sci USA 86:5153–5187.

Monyer H, Sprengel R, Schoepfer R, Herb A, Higuchi M, Lomeli H, Burnashev N, Sakmann B, Seeburg PH (1992) Heteromeric NMDA receptors: molecular and functional distinction of subtypes. Science 256:1217–1221.

Moriyoshi K, Masu M, Ishii T, Shigemoto R, Mizuno N, Nakanishi S (1991) Molecular cloning and characterization of the rat NMDA receptor. Nature 354:31–37.

Morrison JH (1993) Differential vulnerability, connectivity, and cell typology. Neurobiol Aging 14:51–54.

Morrison JH, Magistretti PJ, Benoit R, Bloom FE (1984) The distribution and morphological characteristics of the intracortical VIP-positive cell: an immunohistochemical analysis. Brain Res 292:269–282.

Nakanishi N, Axel R, Shneider NA (1992) Alternative splicing generates functionally distinct N-methyl-D-aspartate receptors. Proc Natl Acad Sci USA 89:8552–8556.

Nakanishi S (1992) Molecular diversity of glutamate receptors and implications for brain function. Science 258:587–603.

Nicoll A, Larkman A, Blakemore C (1992) EPSPs in rat neocortical pyramidal neurones in vitro are prolonged by NMDA receptor-mediated currents. Neurosci Lett 143:5–9.

Nishigori A, Tsumoto T, Kimura F (1990) Contribution of quisqualate/kainate and NMDA receptors to excitatory synaptic transmission in the rat's visual cortex. Vis Neurosci 5:591–604.

Nowak L, Bregestovski P, Ascher P, Herbert A, Prochiantz A (1984) Magnesium gates glutamate-activated channels in mouse central neurones. Nature 307:462–465.

Nudo RJ, Jenkins WM, Merzenich MM (1990) Repetitive microstimulation alters the cortical representation of movements in adult rats. Somatosens Mot Res 7:463–483.

Parnavelas JG, Papadopoulos GC, Cavanagh ME (1988) Changes in neurotransmitters during development. In: Cerebral cortex, Vol 7,

Development and maturation of cerebral cortex (Peters A, Jones EG, eds), pp 177–203. New York: Plenum.

Peters A (1984) Chandelier cells. In: Cerebral cortex, Vol 1, Cellular components of the cerebral cortex (Peters A, Jones EG, eds), pp 361–380. New York: Plenum.

Peters A, Palay SL, Webster HD (1991) The fine structure of the nervous system, 3d ed. New York: Oxford UP.

Petralia RS, Wenthold RJ (1992) Light and electron immunocytochemical localization of AMPA-selective glutamate receptors in the rat brain. J Comp Neurol 318:329–354.

Pons TP, Garraghty PE, Ommaya AK, Kaas JH, Taub E, Mishkin M (1991) Massive cortical reorganization after sensory deafferentation in adult macaques. Science 252:1857–1860.

Riche D, Lanoir J (1978) Some claustro-cortical connections in the cat and baboon as studied by retrograde horseradish peroxidase transport. J Comp Neurol 177:435–444.

Rogers SW, Hughes TE, Hollmann M, Casic GP, Deneris ES, Heinemann S (1991) The characterization and localization of the glutamate receptor subunit GluR1 in the rat brain. J Neurosci 11:2713–2724.

Rothman SM, Olney JW (1987) Excitotoxicity and the NMDA receptor. Trends Neurosci 10:299–302.

Saint Marie RL, Peters A (1985) The morphology and synaptic connections of spiny stellate neurons in monkey visual cortex (area 17): a Golgi-electron microscopic study. J Comp Neurol 226:213–235.

Salt TE (1986) Mediation of thalamic sensory input by both NMDA receptors and non-NMDA receptors. Nature 322:263–265.

Salt TE, Eaton SA (1989) Function of non-NMDA receptors and NMDA receptors in synaptic responses to natural somatosensory stimulation in the ventrobasal thalamus. Exp Brain Res 77:646–652.

Shima K, Tanji J (1993) Involvement of NMDA and non-NMDA receptors in motor task–related activity in the primary and secondary cortical motor areas of the monkey. Cereb Cortex 3:330–347.

Shirokawa T, Nishigori A, Kimura F, Tsumoto T (1989) Actions of excitatory amino acid antagonists on synaptic potentials of layer II/III neurons in the cat's visual cortex. Exp Brain Res 78:489–500.

Siegel SJ, Brose N, Janssen WG, Gasic GP, Jahn R, Heinemann SF, Morrison JH (1994) Regional, cellular and ultrastructural distribution of the glutamate receptor subunit NMDAR1 in monkey hippocampus. Proc Natl Acad Sci USA 91:564–568.

Somogyi P, Cowey A (1984) Double bouquet cells. In: Cerebral cortex, Vol 1, Cellular components of the cerebral cortex (Peters A, Jones EG, eds), pp 337–360. New York: Plenum.

Steward O, Tomasulo T, Levy WB (1990) Blockade of inhibition in a pathway with dual excitatory and inhibitory action unmasks a capability for LTP that is otherwise not expressed. Brain Res 516:292–300.

Sugihara H, Moriyoshi K, Ishii T, Masu M, Nakanishi N (1992) Structures and properties of seven isoforms of the NMDA receptor generated by alternative splicing. Biochem Biophys Res Commun 185:826–832.

Sutor B, Hablitz JJ (1989) EPSPs in rat neocortical neurones *in vitro*. II. Involvement of N-methyl-D-aspartate receptors in the generation of EPSPs. J Neurophysiol 61:621–634.

Thomson AM (1986) A magnesium-sensitive postsynaptic potential in rat cerebral cortex resembles neuronal responses to N-methylaspartate. J Physiol (Lond) 370:531–549.

Tigges M, Bos J, Tigges J, Bridges E (1977) Ultrastructural characteristics of layer IV neuropil in area 17 of monkeys. Cell Tissue Res 182:39–59.

Tsumoto T, Haghihara H, Sato H, Hata Y (1987) NMDA receptors in the visual cortex of young kittens are more effective than those of adult cats. Nature 327:513–514.

Valverde F (1985) The organizing principles of the primary visual cortex in the monkey. In: Cerebral cortex, Vol 3, Visual cortex (Peters A, Jones EG, eds), pp 207–257. New York: Plenum.

van Brederode JFM, Mulligan KA, Hendrickson AE (1990) Calcium-binding proteins as markers for subpopulations of GABAergic neurons in monkey striate cortex. J Comp Neurol 298:1–22.

Vickers JC, Huntley GW, Edwards AM, Moran T, Rogers SW, Heinemann SF, Morrison JH (1993) Quantitative localization of AMPA/kainate and kainate glutamate receptor subunits in neurochemically identified subpopulations of neurons in the prefrontal cortex of the macaque monkey. J Neurosci 13:2982–2992.

Welker E, Soriano E, Dorfl J, Van der Loos H (1989) Plasticity in the barrel cortex of the adult mouse: transient increase of GAD-immunoreactivity following sensory stimulation. Exp Brain Res 78:659–664.

Wenthold RJ, Yokotani N, Doi K, Wada K (1992) Immunochemical characterization of the non-NMDA glutamate receptor using subunit-specific antibodies. J Biol Chem 267:501–507.

White EL (1989) Cortical circuits. Boston: Birkhäuser.

White EL, Czeiger D (1991) Synapses made by axons of callosal projection neurons in mouse somatosensory cortex: emphasis on intrinsic connections. J Comp Neurol 303:233–244.

Williams SM, Goldman-Rakic PS, Leranth C (1992) The synaptology of parvalbumin-immunoreactive neurons in the primate prefrontal cortex. J Comp Neurol 320:353–369.

Winfield DA, Brooke RNL, Sloper JJ, Powell TPS (1981) A combined Golgi-electron microscopic study of the synapses made by the proximal axon and recurrent collaterals of a pyramidal cell in the somatic sensory cortex of the monkey. Neuroscience 6:1217–1230.

Wong-Riley M (1979) Changes in the visual system of monocularly sutured or enucleated cats demonstrable with cytochrome oxidase histochemistry. Brain Res 171:11–28.

Young AB, Fagg GE (1990) Excitatory amino acid receptors in the brain-membrane binding and receptor autoradiographic approaches. Trends Neurosci 11:126–133.